Contents lists available at ScienceDirect

Biomaterials and Biosystems

journal homepage: www.elsevier.com/locate/bbiosy

Rise of tissue- and species-specific 3D bioprinting based on decellularized extracellular matrix-derived bioinks and bioresins

Laura Elomaa [a,*], Ahed Almalla [a], Eriselda Keshi [b], Karl H. Hillebrandt [b,c], Igor M. Sauer [b,d], Marie Weinhart [a,d,e]

[a] *Institute of Chemistry and Biochemistry, Freie Universität Berlin, Takustr. 3, Berlin 14195, Germany*
[b] *Experimental Surgery, Department of Surgery, CCM|CVK, Charité – Universitätsmedizin Berlin, Augustenburger Platz 1, Berlin 13353, Germany*
[c] *Berlin Institute of Health at Charité – Universitätsmedizin Berlin, BIH Biomedical Innovation Academy, BIH Charité Clinician Scientist Program, Charitéplatz 1, Berlin 10117, Germany*
[d] *Cluster of Excellence Matters of Activity, Image Space Material funded by the Deutsche Forschungsgemeinschaft (DFG, German Research Foundation) under Germany's Excellence Strategy – EXC 2025, Germany*
[e] *Institute of Physical Chemistry and Electrochemistry, Leibniz Universität Hannover, Callinstr. 3A, Hannover 30167, Germany*

ARTICLE INFO

ABSTRACT

Thanks to its natural complexity and functionality, decellularized extracellular matrix (dECM) serves as an excellent foundation for creating highly cell-compatible bioinks and bioresins. This enables the bioprinted cells to thrive in an environment that closely mimics their native ECM composition and offers customizable biomechanical properties. To formulate dECM bioinks and bioresins, one must first pulverize and/or solubilize the dECM into non-crosslinked fragments, which can then be chemically modified as needed. In bioprinting, the solubilized dECM-derived material is typically deposited and/or crosslinked in a layer-by-layer fashion to build 3D hydrogel structures. Since the introduction of the first liver-derived dECM-based bioinks, a wide variety of decellularized tissue have been employed in bioprinting, including kidney, heart, cartilage, and adipose tissue among others. This review aims to summarize the critical steps involved in tissue-derived dECM bioprinting, starting from the decellularization of the ECM to the standardized formulation of bioinks and bioresins, ultimately leading to the reproducible bioprinting of tissue constructs. Notably, this discussion also covers photocrosslinkable dECM bioresins, which are particularly attractive due to their ability to provide precise spatiotemporal control over the gelation in bioprinting. Both in extrusion printing and vat photopolymerization, there is a need for more standardized protocols to fully harness the unique properties of dECM-derived materials. In addition to mammalian tissues, the most recent bioprinting approaches involve the use of microbial extracellular polymeric substances in bioprinting of bacteria. This presents similar challenges as those encountered in mammalian cell printing and represents a fascinating frontier in bioprinting technology.

1. Introduction

Decellularized extracellular matrix (dECM) is a highly attractive biomaterial used in the field of bioprinting for creating engineered living materials [1] and tissue constructs [2]. In the realm of regenerative medicine, bioprinting human tissues using eukaryotic cells and matrices from mammal origin is particularly important. dECM plays a crucial role by mimicking the composition structure of natural human tissue environments, offering valuable bioinstructive cues to the hosted cells [3]. In particular, tissue-specific dECM can guide the differentiation and function of stem cells related to that particular tissue [4]. When cells are removed through decellularization, the ECM fibrous network containing structural and functional molecules, such as glycosaminoglycans (GAGs), proteoglycans, glycoproteins, cytokines, and growth factors, is ideally preserved. However, depending on the decellularization method, some ECM components are typically lost, underscoring the need for careful method selection. With key ECM components preserved, dECM is gaining recognition as a highly cytocompatible, bioinstructive, and adaptable material for bioprinting of cell-laden tissue constructs [5]. To bioprint dECM hydrogels, one can either extrude dECM-based cell-containing bioink and crosslink it physically or chemically layer-by-layer, or employ photocrosslinkable dECM-based bioresin that

is covalently crosslinked when exposed to light in a vat. Both printing techniques yield multi-layered 3D constructs defined by their digital computer-aided design (CAD) model [6,7]. Beyond cell-containing bioinks or bioresins, the dECM can also be formulated into acellular biomaterial inks or resins, which can be 3D printed into hydrogels, with cell seeding taking place afterward [8]. This approach offers the advantage of creating more complex structures without concerns about cell viability during the printing process. However, achieving homogeneous tissue growth within these structures can be more challenging when compared to constructs bioprinted using cell-containing bioinks and bioresins.

In this review, we provide a deep insight into the formulation of dECM-based bioinks, bioresins, and biomaterial inks and resins derived from mammalian tissue. We also provide a comprehensive overview of the current state of dECM bioprinting. Our scope extends beyond extrusion-based 3D printing as we also explore the vat photopolymerization of chemically modified dECM bioresins, an area that has been overlooked in previous reviews. Towards the end, we also briefly discuss recent advancements in bioprinting of living prokaryotic materials, a topic that has not yet received much attention in literature. Our overarching goal is to offer guidance on efficiently and precisely formulating dECM bioink and bioresin, ensuring their reproducible use in bioprinting. We also discuss the need for standardization in assessing the bioactive and bioprinting properties of dECM in the future. Fig. 1 illustrates the entire workflow involved in tissue-derived dECM bioprinting, spanning from the initial isolation and decellularization of native tissue to the solubilization and standardized formulation of the dECM materials, ultimately culminating in the (bio)printing of predefined dECM tissue constructs.

2. Decellularization of tissue ECM

2.1. Physical and enzymatic methods

Whenever considering the transplantation of tissue-engineered dECM-based constructs, it is crucial to completely remove species-specific cellular antigens from the matrix to ensure the safe application [9]. While there are no universal guidelines for decellularized materials, according to Crapo et al. [10]. successfully decellularized ECM should contain no more than 50 ng deoxyribonucleic acid (DNA)

per milligram of dry dECM. Additionally, the DNA fragments should be smaller than 200 base pairs to avoid triggering an immune response, and there should be no visible nuclear components within the dECM [11].

Decellularization of tissue ideally involves gentle yet thorough cell removal, resulting in an acellular dECM with its composition and bioactivity preserved. There are primarily three approaches for cell removal, including physical, biochemical, and chemical methods. The physical methods commonly involve freeze/thaw cycles, direct pressure, sonication, or mechanical agitation, all of which break down cell membranes, causing cell lysis. The lysed cellular components can be afterwards removed, for instance, by flushing with aqueous surfactant solutions [12,13]. In the biochemical decellularization, on the other hand, enzymatic agents, such as deoxyribonuclease (DNAse), ribonuclease (RNAse), and proteases, are frequently used. These enzymes weaken the adhesions between cells and ECM by disrupting cell membranes. Trypsin is a commonly used protease that is often combined with ethylenediaminetetraacetic acid (EDTA) chelator in enzymatic decellularization [14]. Since enzymes can be inefficient when used for a short duration and potentially destructive when applied for a prolonged time, they are often combined with chemical agents to improve their efficacy [14].

2.2. Chemical methods

Chemical decellularization of tissue ECM can be accomplished in two primary ways, including perfusion of decellularization medium through the inherent vessels in tissue or incubation and stirring the tissue in this medium. Triton™ X-100, a commonly used nonionic detergent, is frequently employed for chemical decellularization. It disrupts cellular lipid-lipid and lipid-protein interactions while preserving protein-protein interactions, leading to cell separation and the release of cytoplasmic materials through cell lysis [15]. It is typically used in various concentrations ranging from 0.1% to 5%, either on its own or in combination with trypsin/EDTA or sodium dodecyl sulfate (SDS) [16,17]. SDS is the most frequently used ionic detergent that is typically applied in concentrations between 0.1% and 2%. It effectively disrupts cellular membranes and denaturates proteins, solubilizing both cytoplasmic and nuclear cell membranes and effectively removing cellular material from tissues [16,18,19]. However, prolonged treatment with SDS can result in significant disruption of ECM macromolecules [17]. Another commonly
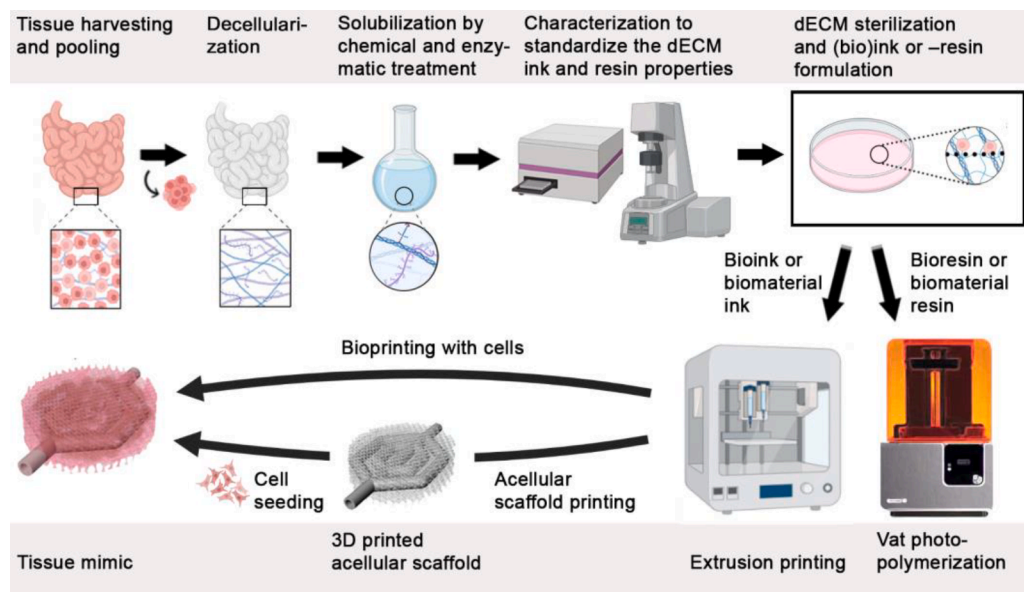

Fig. 1. Schematic presentation of the workflow for bioprinting of dECM-based tissue constructs, including the isolation of human or animal-derived tissue, its decellularization, solubilization, and further formulation into a printing material and finally, 3D printing.

used ionic detergent is sodium deoxycholate (SDC), which comprises a sodium sulfate head group on a steroid backbone. Like SDS, SDC can also effectively solubilize cell membranes. Because of more efficient removal through subsequent washing compared to SDS, dECM obtained using SDC has been shown to support higher metabolic activity of cells [20]. However, SDC-based protocols typically require a subsequent treatment with DNAse to reduce residual DNA levels below an immunogenic threshold [21].

Exposure to decellularization agents inevitably causes some degree of damage to ECM. In a comparative study by Fernández-Pérez et al. [22]. porcine cornea was decellularized using either 0.1% SDS, 1% Triton™ X-100, or five freeze (−80 °C)/thaw cycles. While SDS efficiently removed cells, it resulted in the lowest sulfated GAGs (sGAGs) content and the slowest hydrogel formation. Moreover, the dECM showed cytotoxicity to human corneal stromal cells. Triton and freeze/thaw cycles preserved ECM components better, while the cell removal was not as efficient as with SDS. Jeong et al. [16]. compared the effects of various detergents on the composition and cell compatibility of porcine liver-derived dECM bioinks, finding that SDS and SDC severely damaged GAGs and elastin proteins. In contrast, Triton™ X-100 was less damaging but showed the poorest decellularization. The bioinks obtained using Triton™ X-100 in combination with ammonium hydroxide preserved the ECM content best and exhibited the fastest gelation.

Comparing various decellularization methods is challenging because the reported effects on tissue structure and composition often contradict each other. The absence of systematic studies and standardized processing protocols makes it difficult to provide definitive guidelines for selecting the decellularization method or agent for a certain tissue type. The ideal protocols often combine different decellularization methods and agents, each optimized with specific exposure times. Since dECM-based bioprinting materials are eventually fully solubilized, and there is no need to preserve anatomic architecture of the tissues, incubating the small, precut tissue pieces in decellularization medium, typically in SDS and Triton™ X-100, often ensures the most efficient decellularization.

Even though the source DNA is removed from dECM, the choice of animal species remains significant, as it greatly impacts the amount of tissue that can be obtained. For bioprinting, homogeneous material on a gram scale is required, which is why small animals like rodents are not an ideal choice. Instead, porcine tissue is often preferred, as it provides a larger quantity of tissue and shares known similarities with human tissue [23]. Although the age and health of the source animal can significantly affect the processing of the tissue, this aspect has not been systematically studied. Based on our experience, tissue from older animals may require longer or more intensive decellularization and digestion processes, potentially leading to damage to biomolecules. Additionally, certain diseases, such as fibrosis and cancer, can make the tissue stiffer [24] , which can also pose challenges during the processing steps.

3. Preparing tissue-derived dECM for use in bioinks and bioresins

3.1. Solubilization of tissue dECM via enzymatic digestion

To formulate a bioprinting material from tissue dECM, the first step is to break it down into smaller components to make it soluble in an aqueous cell medium. As the thermo-gelling properties of tissue dECM hydrogels rely on the self-assembly of collagen, selecting an the right solubilization protocol is crucial to avoid adversely affecting its gelling potential later on. The solubilization of dECM is greatly facilitated by first cutting or grinding the tissue into smaller pieces to achieve a homogeneous and deformable 3D printing material. Typically, the dECM is pulverized by initially shock-freezing the wet dECM using liquid nitrogen and then cryo-grinding it, either with a grinding mill or with a pestle and a mortar. Subsequently, the dECM powder can be either directly

mixed with a liquid phase to create a slurry or a paste or, preferably, solubilized through enzymatic digestion. After the enzymatic digestion, the material can be further homogenized and centrifuged to remove any undigested dECM from the solution. Following this, low-molecular weight compounds can be removed from the solution by dialysis, and the material can be stored in a lyophilized and sterilized state, ready for later formulation as a bioink or bioresin. This process is illustrated in Fig. 2.

To fully solubilize a dECM matrix, the cut or pulverized dECM can be treated with various enzymes, with pepsin being the most commonly used, as initially reported by Voytik-Harbin et al. [25]. Pepsin is an endoproteolytic enzyme originally extracted from porcine stomach. It exhibits its highest activity at a low pH, typically below 3. Pepsin digestion involves removal of short non-helical telopeptide regions of tropocollagen, effectively cleaving the crosslinks between tropocollagen units without damaging the collagen triple helical structure. Peptide bonds are preferentially cleaved next to aromatic amino acids such as phenylalanine, tyrosine, and tryptophan [26]. The typical digestion solution contains 0.1% of pepsin in an acidic medium, and the dECM is stirred for 24–72 h at RT [27]. The completion of the digestion, indicated by the absence of visible particles in the solution, can be determined through visual inspection. If pepsin digestion is incomplete, the digestive solution needs to be filtered or centrifuged before use to ensure a high degree of homogeneity. Following digestion, the pepsin is irreversibly deactivated by raising the pH above 5–6.

In a recent study, we explored alternative enzymes to pepsin for solubilizing porcine liver for bioink formulation, including plant-derived papain and bacterial-derived α-amylase and collagenase [28]. Among the investigated enzymes, only pepsin- and papain were successful in digesting dECM to later yield stable hydrogels. Papain, a proteolytic enzyme extracted from papaya fruit seeds, digests dECM by cleaving the non-helical telopeptides of collagen, preferably after the lysine or arginine residues at its N-terminus [29]. In our study, the liver dECM was digested using 0.5 mg papain (30 K USP) per 10 mg of dry dECM for 48 h at pH 5.5 and RT. The resulting dECM digest exhibited good gelation properties, and its rheological and cell adhesion properties were comparable to pepsin-solubilized dECM digests. This made papain an attractive and cost-effective alternative to pepsin for large-scale dECM digestion. Being a plant-derived compound, papain has the potential to replace pepsin especially when working with human tissue-derived dECM for regenerative medicine, where avoiding animal-derived compounds is favorable. Collagenase, on the other hand, digests collagen differently. It breaks down the α-chains of the collagen triple helix into small fragments. Consequently, dECM preparations solubilized with collagenase in our study exhibited significantly reduced viscosity and did not have the ability to form gels [28]. In another study, Jia et al. [30]. chemically modified collagenase-solubilized (2 mg/mL, 24 h, RT) decellularized porcine auricular cartilage using methacrylic anhydride and used this for photocrosslinking-assisted bioprinting together with gelatin methacrylamide (GelMA). According to proteomics analysis, the collagenase treatment preserved many essential ECM components.

Unlike the proteolytic enzymes, α-amylase works by cleaving glycosidic bonds of sugars that are covalently linked between collagen molecules, rather than breaking peptide bonds. This results in the rearrangement and solubilization of well-preserved collagen fibrils [29]. α-amylase has been used to solubilize decellularized human adipose tissue, porcine dermis tissue, and porcine left ventricle using 0.3% α-amylase per dry dECM in slightly acidic environment in 0.22 M NaH_2PO_4 at pH 5.4 [31]. The digestive suspension was agitated for 72 h at RT and centrifuged, after which the pellet was extracted with 0.2 M acetic acid. The dECM that has been digested with α-amylase allowed for the creation of stable foams and microcarriers through lyophilization and rehydration [31]. In our study, we found that the α-amylase digestion of porcine liver dECM preserved the sGAG content better than pepsin and papain digestion. However, the overall digestion efficiency

Fig. 2. A schematic presentation of typical steps in the dECM solubilization to make the material ready for the bioink or bioresin formulation.

was lower, and the resulting gelation properties were impaired [28].

3.2. Chemical modification to yield photocrosslinkable dECM

After solubilizing the dECM, it can be directly used for extrusion bioprinting, where gelation occurs through the physical process of fibrillogenesis at physical conditions (37 °C and pH 7.4). However, when the material is intended for use as a photocrosslinkable bioresin, the dECM polymers are typically chemically functionalized with double bond-containing moieties [32–34]. This modification allows for the covalent crosslinking of the dECM using light, enhancing the strength of the resulting hydrogels and improving their handling. To date, dECM has primarily been functionalized with double bond-containing methacryl groups. For example, Visser et al. [35] and Rothrauff et al. [36] functionalized dECM derived from tendon-, cartilage-, and meniscus-derived with methacrylic anhydride (MAAH) and then photocrosslinked them into hydrogels mixed with GelMA, albeit without applying the material in 3D printing. Furthermore, MAAH has been used by Ali et al. [37] to methacrylate kidney-derived dECM (259 wt-% of MAAH to dECM, pH 8–9 for 2 d, degree of functionalization (DOF) 80%) and by Kim et al. [38] to methacrylate porcine and skeletal muscle tissue-derived dECM (34.5–103.5 wt-% of MAAH to dECM, pH 8–9 at 4 °C for 2 d, DOF 20–80%). Both groups formulated extrudable inks by mixing the dECM methacrylamide with gelatin, hyaluronic acid, and glycerol or with poly(vinyl alcohol). Similarly, Visscher et al. [34] methacrylated porcine auricular cartilage dECM (207 wt-% of MAAH to dECM, pH 8–9 at 4 °C for 2 d, DOF 71%) for extrusion bioprinting. As additions to these extrudable bioinks, we have synthesized dECM methacrylamide for multi-layer vat photopolymerization. This was achieved by sequential adding of MAAH to rat liver dECM (31 wt-% of MAAH to dECM, pH 9.7 at RT for 1 d, DOF 98%) [39] and porcine small intestine (103 wt-% of MAAH to dECM, pH 9 at RT for 3 h, DOF 88%), [32] resulting in biomaterial resins suitable for the vat photopolymerization.

Beside methacrylic anhydride, Kiyotake et al. [33] used glycidyl methacrylate (GMA) for functionalization of devitalized, solubilized porcine articular cartilage. They applied GMA in a 20-molar excess to ECM and allowed it to react at RT for 6 d. While MAAH functionalized both amine and hydroxyl groups, resulting in the formation of methacrylamides and methacrylates, respectively, GMA resulted in the formation of only methacrylates. This different in functionalization led to clear variations in material properties. The DOF with MAAH had an impact on extrusion bioprinting. The lowest DOF (0.4 mmol/g) resulted in the best printable ECM material, while higher DOFs led to nozzle clogging during bioprinting. The ECM with the highest DOF (1.1 mmol/g) was not printable because of its high viscosity. More recently, they functionalized devitalized cartilage ECM using pentenoic anhydride to achieve faster photocrosslinking through thiol-ene click chemistry compared to their methacrylated ECM [40].

3.3. Sterilization or disinfection of tissue dECM

Ensuring the reliable and effective sterilization or disinfection of dECM is crucial when translating bioprinted dECM to clinical practice

and using it as *in vitro* cell culture material. Unlike biomaterial scaffolds or medical devices that can be sterilized just before use or storage, dECM-based inks and resins should be decontaminated before they are mixed with cells [41]. The decontamination process should effectively sanitize bioinks while causing minimal damage, as the regenerative properties of dECM may be compromised by potential biochemical, biomechanical, or structural changes [5]. The general mechanism of most sterilization and disinfections methods involves denaturating proteins and altering nucleobases in microbial contaminants, which may also affect the dECM components. Table 1 provides an overview of the sterilization and disinfection methods that have been applied to dECM or dECM components, along with their respective advantages and disadvantages in bioink and bioresin development. In current literature, the most commonly used method involves immersing of dECM in per-acetic acid solution, which is convenient as it does not require special equipment. However, it is crucial to thoroughly wash out the peracetic acid from the dECM by consecutive dialysis in sterile water to eliminate any toxic compounds from the material. In our experience, disinfection of chopped lyophilized dECM using ultraviolet (UV) light is a straightforward method that successfully prevents bacterial growth in cell culture experiments.

4. Bioprinting techniques and gelation methods of solubilized tissue dECM

3D printing has evolved from 2D inkjet and laser printing techniques into layer-by-layer processes that enable the fabrication of predefined 3D constructs. The journey from the introduction of stereolithography (SLA) as the first commercial 3D printing technique in 1986 [50] to the early attempts to print cells with modified inkjet printers [51] took nearly two decades. Since 2003, various bioprinting techniques, including extrusion- and photocrosslinking-based bioprinting methods, have been used to create a wide range of cell-laden bioinks, and increasingly, solubilized dECM materials have been involved [5]. Extrusion 3D printing has emerged as a prominent technique in dECM bioprinting, primarily because it allows for the use of solubilized dECM without the need for any chemical modifications. In extrusion printing, dECM bioink is extruded through a nozzle onto a platform or supporting media using mechanical or pneumatical force. The bioink can then be crosslinked thermally or, if additional materials are mixed with dECM, through ionic interactions or exposure to light. Solubilized dECM from various sources, such as cartilage, heart, adipose, and skin tissue, has been extensively utilized for bioprinting [34,52,53]. Bioinks made solely from dECM without additives or chemical modification rely on the thermosensitive physical gel formation of neutral dECM solution at elevated temperatures. This allows extrusion of the bioink at RT through a nozzle onto a heated printing platform. At 37 °C, the hydrogel formation is induced by collagen fibrillogenesis. During this entropy-driven self-assembly process, collagen begins to lose water and aggregates, burying the hydrophobic residues within the fibrils, leading to gel formation [54].

While the extrusion printing remains the primary technique for dECM bioprinting, there is a growing interest in alternative methods that offer improved printing precision and more stable dECM constructs. One

Table 1

Sterilization and disinfection techniques for solubilized dECM powders or hydrated dECM preparations thereof.

Sterilization technique		Advantages	Disadvantages	Refs.
Irradiation	Gamma irradiation	Non-thermal, quick effect, and nontoxic. Excellent penetration in biomaterials.	High cost. Induces crosslinking and/or chain scission. Potential changes in rheological properties. Not broadly accessible.	[42]
	UV irradiation	Easy, cost-effective, simple safety requirements, and applicable in routine laboratory work.	Denatures proteins at high doses. Poor penetration.	[43]
Steam	Autoclaving (saturated steam)	Simple, fast, and low-cost. No toxic residues. Broadly accessible.	Causes degradation or chemical changes leading to reduced viscosity and mechanical properties.	[44]
Filtration	Sterile filtration ($\leq$ 0.22 μm membrane)	Simple, safe, fast, and non-thermal. No toxic residues and cost-effective. Broadly accessible.	Only for digested dECM and not efficient for high molecular weight polymers/components. Causes reduction in rheological properties and a major loss of material.	[44]
Wet chemical	Peracetic acid (0.05–0.5 %)	Easy, efficient, and cost-effective.	Oxidative and acidic residuals left in dECM that require careful purification.	[28, 45–47]
	Ethanol (60 % −80 %)	Easy, simple safety requirements, and broadly accessible.	Ineffective in killing all microorganisms.	[48]
Gas treatment	Ethylene oxide (EtO)	Applicable to heat and moisture-sensitive biomaterials. Efficient microorganism inactivation and good penetration in materials.	High safety requirements and high cost. Toxic, flammable, and carcinogenic gas. Long aeration cycle is necessary.	[43,44]
	Supercritical carbon dioxide (scCO$_2$)	Applicable to heat and moisture-sensitive biomaterials. Green and sustainable technique. High penetration properties. Nontoxic, non-flammable, and non-reactive.	Under mild operating conditions (e.g., low temperature and pressure) does not promote complete bacterial spore inactivation. Not applicable to routine laboratory work.	[43,49]

such method is vat photopolymerization, a 3D printing technique that creates of dECM 3D constructs by photocrosslinking a liquid photoinitiator-containing resin into well-defined geometries [7]. This process can be achieved using a computer-controlled laser beam in SLA or a projector in digital light processing (DLP) or a liquid crystal display (LCD) for photocrosslinking subsequent resin layers [7]. Vat photopolymerization offers several advantages, including higher resolution compared to extrusion printing. The resolution is primarily limited by the laser width or the pixel size, being as good as tens of micrometers, rather than the size of a printing head or the printing speed and pressure. Additionally, the material waste is often minimized, as in a typical bottom-up vat photopolymerization printer, all the resin can be used until the last drop. However, unlike extrusion printing, which relies on the thermosensitive gelation of a dECM hydrogel, vat photopolymerization requires either free-radical-initiated photocrosslinking of double bond-containing, functionalized dECM [32,39,55–57] or ruthenium-initiated photocrosslinking of unfunctionalized dECM [58]. Therefore, additional chemical modification of the dECM and/or use of photoinitiating compounds is necessary for the covalent crosslinking of the hydrogels. In the photopolymerization process, the photoinitiator, when used, absorbs light in either the UV or visible light range, becoming excited into a high-energy radical state. These radicals then react with the functionalized dECM polymers, initiating the crosslinking [32]. In the case of ruthenium chemistry, the tyrosine side groups of dECM are oxidized and converted into radicals, which are quenched through the formation of intermolecular covalent dityrosine bonds [58]. Careful consideration must be given to the amount of the photoinitiating compound used, as high concentrations of the resulting radicals may negatively impact cell viability.

Beside physical or covalent crosslinking of dECM inks and resins, dECM can mixed with other polymers, such as alginate and GelMA, and crosslinked via material-specific techniques. When mixed with GelMA and photoinitiator, the dECM-containing material can be photocrosslinked, either after extrusion [59,60] or during vat photopolymerization [19]. Alginate, on the other hand, is ionically crosslinkable biopolymer that is commonly used in bioprinting because of its favorable rheological properties. The alginate/dECM composite can be rapidly crosslinked by adding divalent cations, such as Ca^{2+}, to the material [61]. This provides easy control over the crosslinking properties of the bioink.

5. Formulation of tissue dECM-derived bioinks and bioresins

5.1. Bioink and bioresin formulation and cell embedding

To formulate a dECM bioink or bioresin for use in extrusion-based printing techniques or vat photopolymerization, the digested dECM is initially dissolved in a basic or acidic solution and then neutralized before being mixed with cells. It is essential to use the bioink or bioresin immediately after adding the cells to minimize the time the cells spend outside the standard cell culture conditions. The density of cells in dECM bioinks typically ranges from 1 to 50 million cells per milliliter. While the physicochemical properties of cell-laden dECM bioinks have been extensively characterized, there has not been a proper correlation between these properties and cell density. However, as cells occupy a certain volume in the bioink and potentially create physical hindrance between polymer chains, their density can influence factors such as rheological and crosslinking properties [62]. Moreover, cells transform a bioink into a composite material that may behave as a colloidal system and exhibit enhanced shear-thinning behavior [63]. In some cases, high cell densities, up to 100 million cells per milliliter, have been found to slightly increase the viscosity of collagen-based bioinks and reduce both the gelation rate and resulting storage modulus compared to their acellular counterparts [64]. Additionally, the line width of extruded hydrogels has been observed to decrease with the addition of cells, underscoring the importance of cell density for bioink properties. To

prevent potential cell sedimentation and ensure a homogeneous cell distribution during lengthy bioprinting process for clinically relevant applications, careful adjustments of material viscosities are necessary. This can be achieved by altering the dECM concentration or blending dECM with other polymers [61].

5.2. Adjusting the crosslinking density and viscosity

When it comes to bioprinting materials containing living cells, the ideal bioink or bioresin should prioritize both high cell viability and excellent shape fidelity. The range of ideal bioprinting conditions that simultaneously optimize cell viability and printing resolution is referred to as „bioprinting window" [65]. However, these two requirements can be often contradictory, as soft hydrogels that are preferred for good cell viability can be prone to deformation, resulting in decreased shape fidelity [63]. Increasing the stiffness of the hydrogel by using a higher dECM concentration can lead to reduced cell viability, [66] as the increased crosslinking density reduces the mesh size and consequently the free space available for cell proliferation and migration. For example, in a study by Ahn et al., [66] increasing the concentration of porcine skin-derived dECM in the bioink from 1.5 – 2% to 2.5% improved the resolution of the extrusion bioprinting but significantly decreased the viability of mouse NIH3T3 fibroblasts. This highlights the importance of selecting an appropriate dECM concentration, as it strongly influences the key characteristics of a bioprinting material, *i.e.,* the viscosity and crosslinking density.

In extrusion bioprinting, the initial viscosity of the bioink has to be low enough to allow smooth flow through the extrusion head without blockages and to protect the cells from excessive shear stress. After deposition, the bioink should ideally increase its viscosity or solidify to ensure good shape fidelity. Therefore, dECM bioinks with fast crosslinking kinetics or shear-thinning behavior are favorable [65]. Shape-fidelity of low-viscosity dECM bioinks and bioresins can also be improved by printing the material into a supporting bath [67] or by extruding it in combination with ionically crosslinking alginate through a co-axial needle along with an ionic solution [68]. Alternatively, the hydrogel can photocrosslinked *in situ* while photocrosslinkable material is being deposited [69]. Similar to extrusion printing, vat photopolymerization requires the free flow of the dECM bioresin before photocrosslinking, allowing efficient removal of non-crosslinked material from a freshly crosslinked layer to prevent over-crosslinking.

The viscosity of dECM-based bioinks and bioresins depends not only on the dECM concentration but also on the enzymatic digestion time of the dECM [70]. In the early stages of digestion, dECM forms a highly viscous slurry, which gradually decreases in viscosity as more proteins are cleaved [71]. This reduction in viscosity can improve the material flow, but it may come with the cost of cell-compatibility of the resulting hydrogels, as has been reported by Pouliot et al. [27]. In their study, 12 h digestion time of porcine lung dECM resulted in the optimal balance between physical properties and compatibility of the hydrogels with seeded cells. Similarly, in another study by Zhao et al., [71] a longer digestion time for tendon dECM led to lower viscosity, which in extrusion printing impaired the stacking precision of the bioink. Interestingly, the viability of rat bone marrow mesenchymal stem cells bioprinted in the hydrogels was higher in the hydrogels with lower viscosity compared to those with higher viscosity. The optimal digestion time and viscosity requirements vary based on the particular 3D printing technique in use and whether cells are seeded onto the hydrogels or bioprinted within them. It is important to note that the progress of digestion depends on various parameters, including the type and activity of the enzyme, the ratio of enzyme to substrate, pH, agitation speed, and the size of the initial dECM pieces. Because of these variations, the results from different studies may not be directly comparable in terms of digestion time.

5.3. Photoinitiators in dECM resins

In vat photopolymerization, dECM hydrogels are created through photocrosslinking, while in extrusion printing, photocrosslinking can be applied as an optional step after extrusion. Typically 3D printers apply UV-A light (320–400 nm) or visible light, which are both less harmful to the cells compared to higher-energy light with lower wavelengths [72]. The potential harm to encapsulated cells is not primarily from direct light radiation but rather from the high-energy radicals produced during the photocrosslinking. These radicals can lead to oxidative damage to cellular components, particularly DNA [73]. When photoinitiators are used, they must be nontoxic to the encapsulated cells. The cytotoxicity of photoinitiators depends on factors such as their hydrophobicity and the concentration of free radicals they generate. Therefore, selecting the right photoinitiator and controlling its concentration can generally improve cell viability during the bioprinting.

In dECM-based bioresins, three main photoinitiators are commonly used, including Irgacure 2959, [37] lithium phenyl-2,4, 6-trimethylbenzoylphosphinate (LAP) [19,39,48,52], and riboflavin (vitamin B$_2$) [41]. Irgacure 2959 is widely used due to its water-solubility and low cytotoxicity, making it compatible with various cell lines and concentrations [74]. It absorbs light most efficiently between 280 and 320 nm but remains sensitive to light up to the end of the UV spectrum [75]. LAP was developed as a water-soluble photoinitiator with a second absorption peak closer to 400 nm, allowing for crosslinking with visible light [74]. The cell viability using LAP at the concentration of 0.9% has been significantly higher compared to that using Irgacure 2959 after extended bioprinting time [74]. Riboflavin, at a concentration of 0.02 %, has been used for crosslinking dECM constructs with high cell viability [41]. It initiates a photochemical reaction involving active oxygen radicals that promote collagen crosslinking, a concept previously used in dentistry and eye treatments [76]. In addition to these radical-forming photoinitiators, ruthenium complexes have been used for covalent crosslinking of dECM. In the presence of visible light and the electron acceptor sodium persulfate (SPS), the system facilitates the conversion of Ru^{2+} to Ru^{3+}, which then oxidizes tyrosine groups in collagen and other proteins, generating tyrosyl free radicals [58]. This approach at the concentration of $0.2/2 \times 10^{-3}$ M for Ru/SPS has demonstrated the potential for dECM bioprinting, with up to 80% cell viability observed for cardiomyocytes in bioprinted heart dECM [58].

6. Characterization of dECM bioinks and bioresins and bioprinted hydrogels

6.1. Structural and compositional characterization

In the quest for reproducible dECM-based bioinks and bioresins, it is advisable to pool tissue from multiple source animals or patients for the ECM decellularization. This approach helps mitigate biological variability and ensures an adequate supply of material for bioprinting multiple tissue constructs of clinically relevant sizes. Characterizing digested dECM bioprinting materials typically involves several analytical techniques that help monitoring and standardizing these materials. Immunohistochemical staining allows for the visual detection of collagen and elastin, providing insights into the presence of these ECM proteins [16,19,77]. The amount of collagen can be quantitatively assessed using methods like the chloramine-T hydroxyproline assay. Sulfated GAGs in dECM can be quantified through assays such as the dimethylmethylene blue assay [78]. To evaluate the potential bioactivity of dECM, the remaining growth factors can be quantified using enzyme-linked immunosorbent assay (ELISA)-based growth factor arrays [32,37]. The proteomics of native and decellularized ECM can be studied in more detail using liquid chromatography coupled with tandem mass spectrometry (LC-MS/MS). This technique provides extensive compositional data, revealing the presence of specific proteins, such as

collagen, elastin, laminin, and fibronectin in digested dECM [4,32].

To understand how a specific digestion protocol affects the molecular weight of the resulting macromolecules, SDS-polyacrylamide gel electrophoresis (SDS-PAGE) that separates denatured protein fragments by size can be applied [32]. For example, it has been shown using SDS-PAGE that prolonged dECM fragmentation could lead to a decreased relative amount of trimeric collagen and an increased amount of monomeric collagen [27]. Furthermore, the secondary structure of collagen within dECM digests can be studied using Fourier-transform infrared spectroscopy (FTIR) [16]. This method involves comparing FTIR spectra at different stages of processing to uncover any potential changes in collagen's conformation. Collagen has a distinct fingerprint absorption represented by specific bands at wave numbers of 1654, 1548, and 1238 cm^{-1}, while an absorption band at 1048 cm^{-1} can suggest the presence of GAGs in the dECM [16]. Additionally, FTIR-spectroscopy can be used to track the successful removal of toxic SDS residues after decellularization [70]. To further explore the protein's structure, circular dichroism (CD) spectroscopy can be employed. This technique helps characterize both the secondary and tertiary structure of collagen and is capable of detecting potential conformational changes in dECM [67].

In addition to the methods mentioned above, proton nuclear magnetic resonance (^{1}H NMR) can be used to assess the DOF in photo-crosslinkable dECM. The conversion of free primary amine groups to methacrylamide groups can be analyzed following the peak at 2.9 ppm in a ^{1}H NMR spectrum assigned to terminal methylene groups in the lysine side chains in dECM [32,33]. The functionalization can also be measured quantitatively using a colorimetric 2,4,6-trinitrobenzene sulfonic acid (TNBS) assay. This assay relies on a reaction between the free lysine amine groups and TNBS, resulting in a colored compound, which can be measured using a UV–Vis spectrometer at the 346 nm absorbance [32,33]. Furthermore, the conversion of primary amines and hydroxyl groups into methacrylamides and methacrylates, respectively, can be quantified using the ^{1}H NMR by comparing the signals of protons from methacrylamides (around 5.4 −5.7 ppm) and protons of methacrylates (around 5.8–6.0 ppm) to an internal standard, as shown by Kiyotake et al. [33].

6.2. Rheological properties

The key characteristics of dECM-based inks and resins for 3D printing are their rheological properties and gelation kinetics. These properties are crucial because they impact the printing speed and resolution and the shape fidelity and cell viability. The viscosity and viscoelastic properties of dECM both prior to and during the crosslinking can be assessed using a rotating and oscillating rheometer. This approach helps adjusting the material for homogeneous cell encapsulation and bioprinting [16,32,70]. The shear-thinning behavior of dECM bioink, which is an advantageous trait for extrusion-based 3D bioprinting, can be detected as consistent reduction in shear viscosity as the shear rate increases and is caused by progressive macromolecule alignment [65]. Additionally, various other rheological attributes, including flow initiation, post-printing recovery time, and the presence of yield stress, are known to influence the shape fidelity of various bioinks [79–81]. Investigating these properties for dECM-based bioinks and bioresins could offer valuable insights for optimizing these materials for bioprinting applications.

The gelation process of physical dECM hydrogels, which relies on collagen fibrillogenesis, can be monitored turbidimetrically by observing the increasing light scattering of the diluted dECM solution [16]. Additionally, the gelation can be tracked in real-time using a rheometer, where the loss modulus decreases and the storage modulus increases as the temperature is raised to 37 °C [70]. While physically crosslinked dECM constructs form relatively soft hydrogels, chemical photocrosslinking strengthens the material by increasing the crosslinking density. The photocrosslinking kinetics of a dECM resin significantly depends on factors like polymer concentration and can be studied by using a rheometer combined with an *in situ* photocrosslinking light source [32]. In this method, a small amount of resin is positioned between the rheometer plates, and while exposing the material to UV or visible light, the elastic and viscous modulus are measured. The progression of resin crosslinking into a hydrogel is then detected as a decreasing loss modulus and an increasing storage modulus [32].

6.3. 3D printing properties of the dECM materials

In addition to understanding the biochemical composition and rheological and mechanical properties of dECM materials, it is crucial to thoroughly investigate how these materials behave within a 3D printer. In particular, for extrusion printing, factors like the width and height of the extruded lines, which determine the printing resolution, are crucial. These line dimensions are influenced by various factors, such as the size, speed, and pressure of the extrusion head, as well as viscosity of the bioink [16,71]. Typically, as the size and pressure of the extrusion head increase, the line with also increases, reducing the resolution. This can be inspected visually [37]. Furthermore, it is important to assess phenomena like the collapse of a dECM filament and the fusion of adjacent filaments after extrusion, as previously done for other types of (bio)inks [82]. Interestingly, the shape of the extrusion nozzle is known to impact cell survival during bioprinting. For example, a tapered nozzle has been found to allow for the extrusion of dECM bioink at significantly lower pressure compared to a cylindrical needle of the same size, thereby generating less shear stress on the cells [71]. To gain a deeper understanding of the materials' behavior during bioprinting, its shear stress profile can be mapped using computational fluid dynamics simulation and experimental rheological data [61]. This helps in evaluating the stress experienced by cells during the bioprinting. Furthermore, cell viability under different shear stress conditions and potential cell sedimentation can be assessed through fluorescent live/dead cell staining and subsequent microscopy imaging throughout the entire thickness of a bioprinted dECM hydrogel. The sedimentation coefficient can be further quantified based on cell density in different regions of the material [61].

Table 2 provides a summary of commonly used characterization methods for evaluating dECM bioprinting materials and hydrogels. These methods are invaluable for standardizing dECM materials, as they allow for a comprehensive examination of how various processing steps influence material properties.

7. Extrusion printed tissue dECM constructs

7.1. Cardiovascular and muscle tissue constructs

Bioprinted dECM constructs have gained increasing attention in regenerative medicine and as *in vitro* tissue models. The use of dECM in bioprinting can be tracked back to the pioneering work of Professor Dong-Woo Cho at Pohang University in South Korea. In 2014, Pati et al. [86] introduced three bioinks formulated with 3% dECM from various sources, each containing $1–5 \times 10^6$ cells/mL. These bioinks included one with solubilized porcine heart dECM and rat myoblasts, another with human adipose dECM and human adipose-derived stem cells, and a third with porcine cartilage dECM and human inferior turbinate tissue-derived mesenchymal stromal cells. An custom-built 3D printer equipped with two syringe holders was employed to bioprint these cell-laden dECM bioinks at 15 °C, potentially with the polycaprolactone (PCL) support material. The simultaneous printing of a mechanically robust support structure addressed the challenge posed by the low intrinsic stiffness and physical stability of dECM hydrogels. This approach enabled the bioprinting of multilayered non-supported soft heart tissue constructs, PCL-supported hard cartilage tissue, and adipose tissue constructs (Fig. 3A). Within 14 days of cell culture, myoblasts enhanced their functionality in the heart dECM hydrogels and adipose and cartilage cells increased adipogenic and chondrogenic

Table 2

Summary of techniques used for characterization and standardization of dECM-based inks and resins.

Target	Characterization method	Information	Refs.
Biochemical composition	Collagen and elastin assay	Content of specific ECM components	[16,19, 32,66,71, 77]
	GAGs assay		[4,16,19, 32,71, 77].
	Growth factor assay		[32,37]
Chemical composition	SDS-PAGE	Qualitative molecular mass distribution	[32]
	Mass spectroscopy	Proteomics	[4,30,32, 70]
	FTIR	Primary and secondary structure of proteins	[16,70, 71,77]
	CD spectroscopy	Secondary structure of proteins	[32]
	DSC	Denaturation of proteins	[16]
	^{1}H NMR/ TNBS assay	Degree of methacrylation	[32–34, 37,38]
Nanostructure	SEM	Topography	[16,19, 32,70,77]
	AFM	Topography, fiber structure	[28]
Rheological, mechanical, and swelling properties	Turbidimetry	Gelation kinetics	[16]
	Rheology	Viscosity, stiffness	[16,19, 61,70,71]
	Mechanical analyzer	Stiffness, strength, elasticity	[16,19, 77]
	AFM (indentation via contact mode)	Surface stiffness	[32]
	Swelling ratio	Water absorption/ permeability	[16,19, 32,77]
	Degradation study	Enzymatic mass loss	[19,30, 32]
3D printing properties	Optical microscopy	Line/filament dimensions	[16,37, 66,71]
	Optical visualization	Shape fidelity	[16,19, 30,37]
	Weight measurements	Mass flow rate *vs.* pressure	[71]
	Photo-rheology	Photocrosslinking kinetics	[32]
	Computational fluid dynamics	Shear stress simulation	[61]
	Fluorescence microscopy	Cell sedimentation	[61]
Biological properties	Cell culture studies	Cell viability and proliferation, material toxicity	[4,16,19, 32,61,71, 77]
	In vivo experiments	Biocompatibility	[30,77, 83–85]

differentiation in the respective dECM constructs. In 2017, Jang et al. [41] formulated a bioink based on solubilized porcine heart dECM for bioprinting heart patches aimed at myocardial tissue repair (Fig. 3B). This bioink, consisting of 2% heart dECM solution mixed with human cardiac progenitor cells and/or human mesenchymal stem cells (5×10^6 cells/mL in total), vascular endothelial growth factor (10 μL/mL), and vitamin B2 (0.02%) as a photocrosslinker, was bioprinted on PCL support layers. Each layer was crosslinked with UV light. The bioprinted heart patches promoted vascularization and reduced cardiac fibrosis when implanted *in vivo* [41].

An alternative strategy for supporting the physically crosslinked dECM hydrogel, instead of printing a separate support structure, involves blending dECM with a supportive hydrogel material, such as alginate, methacrylated hyaluronic acid (HA-MA), or GelMA to enhance the printability and increase the stiffness [19,60,61]. Basara et al. [60] bioprinted cardiac constructs using a bioink comprising human myocardium-derived dECM (1 mg/mL) mixed either with GelMA (10%)

and human induced pluripotent stem cell (iPSC)-derived cardiomyocytes (20×10^6 cells/mL) or with GelMA (10%), HA-MA (1%), and human cardiac fibroblasts (1×10^6 cells/mL). The addition of HA-MA significantly increased hydrogel stiffness, enabling the *in vitro* modeling of a myocardial infarct boundary. The softer HA-MA-free gel mimicked healthy tissue, while the stiffer HA-MA-containing gel emulated scar tissue. These constructs successfully exhibited heart tissue-like beating [60].

Choi et al. [67] formulated bioinks from porcine muscle dECM (1%) and porcine aorta dECM (3%) for the purpose of volumetric muscle reconstruction with prevascularized tissue. Their study involved the fabrication of three different muscle-derived dECM constructs, all of the same size, each containing human skeletal muscle cells (hSKMs). These constructs included undigested dECM scaffolds reseeded with cells, cell-laden dECM hydrogels (2×10^7 cells/mL) loaded within a PCL anchoring scaffold, and bioprinted cell-laden dECM hydrogels (2×10^7 cells/mL). In a rat model of volumetric muscle loss, the bioprinted constructs exhibited superior myotube formation and *de novo* myofiber regeneration compared to the other samples. Furthermore, in an effort to create prevascularized muscle constructs, a coaxial printing nozzle was used, as depicted in Fig. 3C. In this setup, the aortal dECM mixed with human umbilical vascular endothelial cells (HUVECs) was deposited in the outer shell of the syringe, while the muscle dECM mixed with hSKMs occupied the inner core. Remarkably, the resulting bioprinted multicellular core-shell constructs exhibited enhanced muscle formation and vascularization in a muscle injury model when compared to bioprinted constructs composed of a mixture (1:1) of muscle and aortal bioinks.

7.2. Gastrointestinal and urinary tissue constructs

In addition to cardiac and muscle dECM, liver dECM has been widely used for bioprinting tissue constructs. In 2017, Lee et al. [87] used porcine liver dECM to replicate liver-specific functions. They formulated aqueous porcine dECM bioinks (1.5%) containing human hepatocellular carcinoma (HepG2) cells or human bone marrow-derived mesenchymal stem cells (5×10^6 cells/mL) and used them to create cell-laden constructs, as depicted in Fig. 4A. These constructs were bioprinted using a custom-built hybrid bioprinter. During a 7-day cell culture period of the liver dECM constructs, mesenchymal stem cells differentiated towards hepatic cells, and HepG2 cells exhibited albumin and urea secretion. In 2018, Hiller et al. [88]. bioprinted liver tissue constructs by employing a bioink containing human lung dECM (0–0.2%) derived from a rejected lung transplant, along with alginate (2%), gelatin (3%), 0.03 M CaSO$_4$, and human bipotent hepatic progenitor cells (HepaRG®, 7×10^6 cells/mL). Since human tissue is often in limited supply, except for fat tissue obtained from liposuction, it is frequently blended as a bioactive component with more readily available materials such as alginate and gelatin. The human dECM-containing tissue constructs were bioprinted using a commercial micro-extrusion printer (INKREDIBLE+™, CELLINK) with a 22G needle at 10–20 kPa. Before bioprinting, the alginate in the bioink was initially crosslinked with CaSO$_4$ for 8 min. After bioprinting, the constructs were further solidified in a 0.1 M CaCl$_2$ solution for 5 min. Over a 7-day cell culture period, the cells within the constructs continued to exhibit liver-specific albumin secretion, indicating their potential as liver models. Moreover, these bioprinted constructs served as proof-of-concept humanized adenoviral replication models, demonstrating their suitability for virus replication by showing an increase in the number of infectious particles and adenoviral hexon DNA.

Beside liver tissue constructs, bioprinting has also been applied to create constructs from other internal organs. In 2019, Kim et al. [89] cultured human primary islets (3000 islet equivalents/mL) in a 2% bioink derived from human pancreas dECM collected from a deceased donor. In a 5-day cell culture study, the islets in the dECM secreted more insulin compared to islets in alginate and collagen inks. Furthermore, when islets were co-cultured with HUVECs (1×10^6 cells/mL) in a 1% pancreas dECM bioink for 5 d, they exhibited less central necrosis and
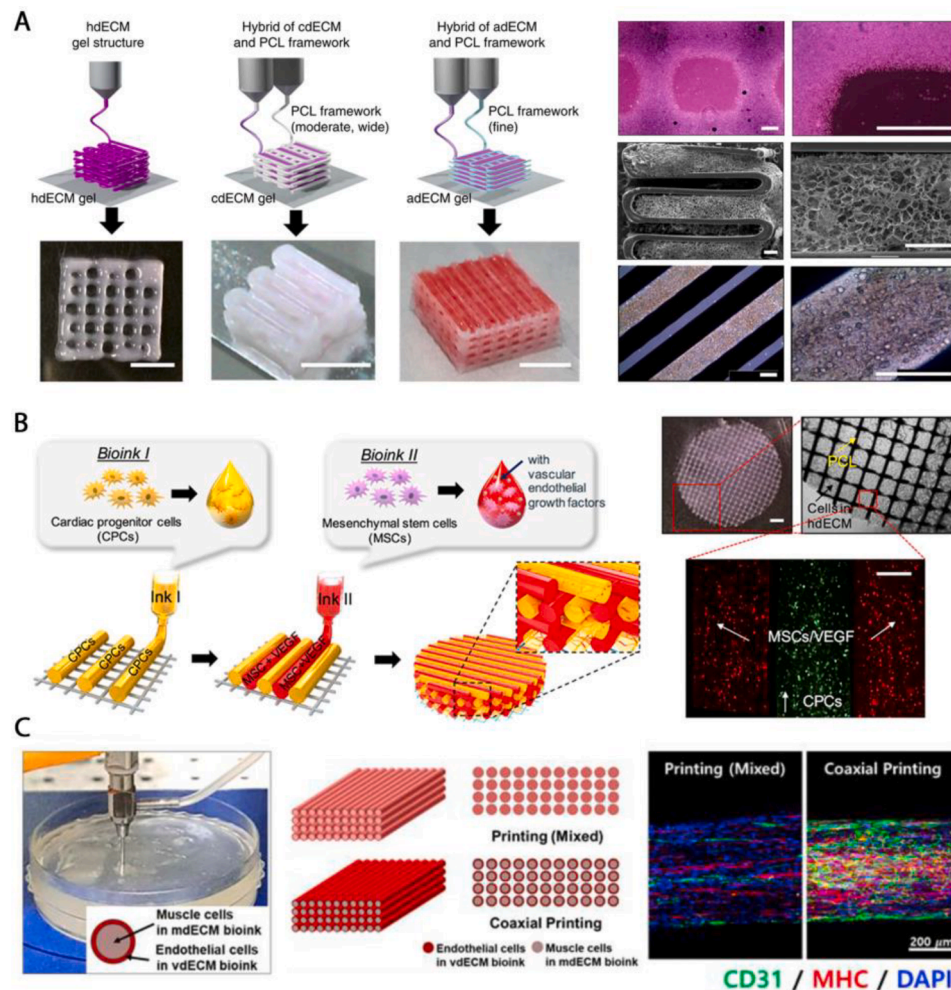
Fig. 3. Extrusion printing of (A) non-supported hydrogels using porcine heart dECM bioink and PCL-supported hydrogels of porcine cartilage and human adipose dECM bioink, [86]. (B) PCL-supported multi-material heart patches of human cardiac progenitor- and mesenchymal stem cell-containing porcine heart dECM bioinks, [41] and (C) prevascularized muscle constructs of muscle cell-containing porcine muscle dECM and HUVEC-containing porcine aortal dECM bioinks using a coaxial printing nozzle [67]. Reproduced with permission from (A) Springer Nature, and (B), (C) Elsevier.

increased insulin secretion compared to their homo-culture. Preliminary extrusion bioprinting of rat islet-laden pancreas-derived dECM bioinks (2,3%) into five-layer constructs shown in Fig. 4B resulted in similar cell viability during a 5-day cell culture when compared to non-printed gels. No mechanical damage to the cells was observed, which was attributed to the optimized printing pressure (20 kPa) and inner nozzle diameter (0.8 mm).

In contrast to chemically unmodified dECM, Ali et al. [37] used methacrylated porcine kidney-derived dECM for extrusion bioprinting of kidney tissue constructs. The solubilized dECM was first functional-ized with methacrylic anhydride, resulting in dECM methacrylamide (3%). This modified dECM was then mixed with gelatin (3%), hyal-uronic acid (0.3%), glycerol (10%), human primary kidney cells (1 × 10^7 cells/mL), and 0.5% of Irgacure 2959 photoinitiator. Renal con-structs (6 × 6 × 12 mm [3]) were bioprinted with an extrusion bio-printer and subsequently photocrosslinked with UV light for 120 s (Fig. 4C). The encapsulated kidney cells retained their kidney-specific phenotype, forming tubular and glomerular structures. Moreover, cell growth was increased compared to control GelMA gels, and hydrolase activity that is essential for amino acid transfer in the kidney was significantly higher in the bioprinted constructs compared to the GelMA constructs.

7.3. Cartilage tissue constructs

Beside soft tissue applications, bioprinting tissue constructs using cartilage-derived dECM has been explored. Jia et al. [30] decellularized and solubilized porcine auricular cartilage and then functionalized it with methacrylic anhydride to create dECM-MA. The dECM-MA was mixed with GelMa (5% each in cell culture medium), LAP photoinitiator (0.25 %), and sacrificial poly(ethylene oxide) porogen (1%, 300 kDa). This emulsion was combined with rabbit chondrocytes (20 × 10^6 cells/mL) and bioprinted into an ear replicate using a multi-syringe 3D-Bioplotter from EnvisionTEC. For alternating layer printing, the cell-laden bioink was extruded at 20 °C, and another high-temperature nozzle was used to fuse-deposit PCL at 65 °C. Each layer was cross-linked with blue light for 10 s. When implanted in nude mice, histology revealed the presence of a cartilage-specific ECM. The porosity of the material, achieved by leaching out the porogen, facilitated the ECM deposition and the formation of a lacunae structure. In contrast, the tissue formed within non-porous hydrogels exhibited only a pericellular matrix scattered in the hydrogel.

Furthermore, Behan et al. [90] used methacrylated solubilized porcine articular cartilage for bioinks (1 or 2% w/v), mixed with gelatin (3.5% w/v) and LAP (0.25% w/v) and loaded with bone marrow mesenchymal stem cells (20 × 10^6 cells/mL). In the extruded 3D con-structs, which were subsequently photocrosslinked using UV light, the
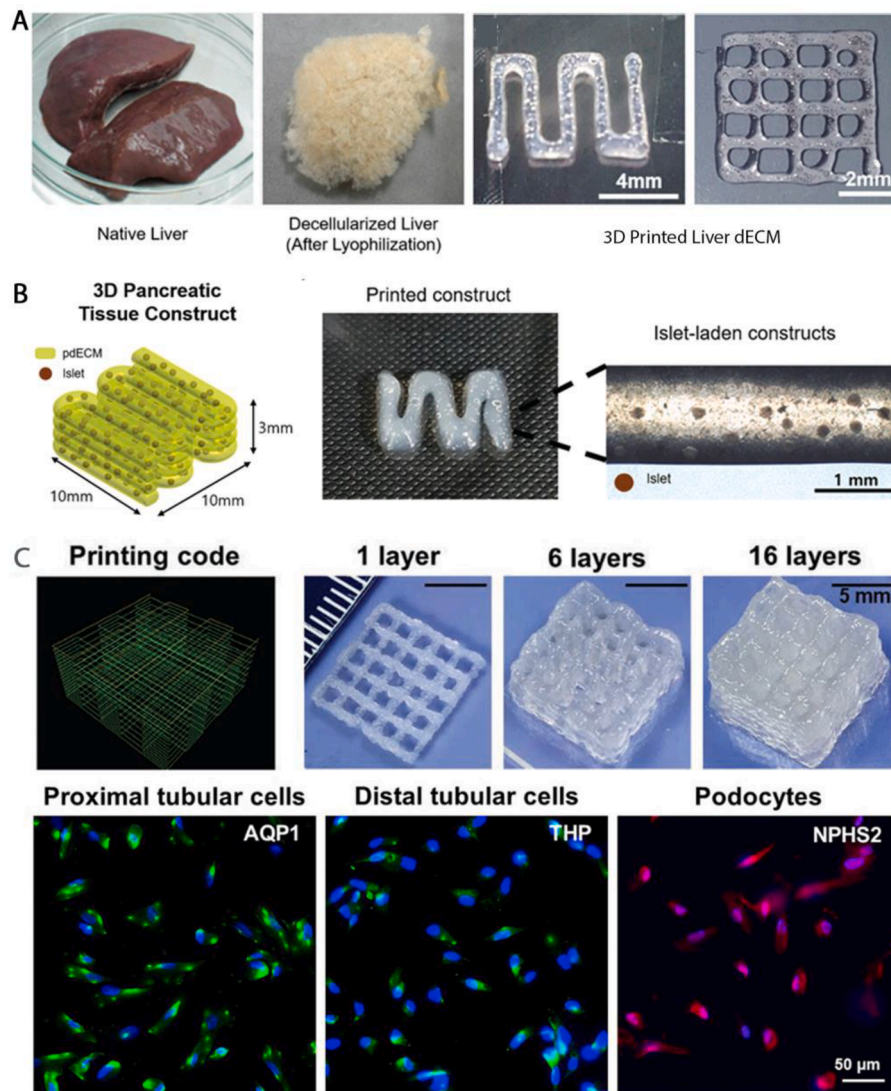
Fig. 4. Extrusion-printed, non-supported hydrogels of (A) porcine liver dECM containing human hepatocellular carcinoma (HepG$_2$) cells or human bone marrow-derived mesenchymal stem cells [87]. and (B) human pancreas dECM containing rat islets after physical crosslinking [89] and (C) methacrylated kidney dECM containing human primary kidney cells after additional covalent crosslinking [37]. Reproduced with permission from (A) American Chemical Society, (B) Royal Society of Chemistry, (C) John Wiley and Sons.

cells exhibited chondrogenesis and generated tissue rich in sulphated glycosaminoglycans and collagens. Additionally, Zhang et al. [91] employed extrusion printing to create ear-shaped cartilage constructs using a 3D Discovery™ printer from Regenhu. Their bioink consisted of goat articular cartilage dECM (0–3%), silk fibroin (SF, 0–7.5 %), PEG (40%, 400 Da), and bone marrow mesenchymal stem cells (1×10^7 cells/mL). The addition of silk fibroin self-assembled β-sheets, enhancing the mechanical stability of the dECM bioink. Cells encapsulated in dECM/SF constructs exhibited a higher mRNA expression level of the cartilage-specific marker gene SOX-9 compared to the neat SF constructs, indicating tissue-specific functionality of the cartilage dECM.

7.4. Other dECM constructs

In addition to the current main application fields, bioprinting has been explored for various other tissue constructs. Kim et al. [45] reported on bioprinting vascularized skin patches using porcine skin-derived dECM inks (1.5%) mixed with human adipose-derived stem cells and human endothelial progenitor cells (2.5×10^5 cells /mL for each). Thin dECM patches were printed with an in-house-built extrusion printer. The resulting *in vitro* vascularized cell-laden patches were

implanted at a dorsal skin wound of 8-week-old male BALB/cA-nu/nu immunodeficient mice. After four days, the study showed enhanced wound closure and neovascularization compared to acellular skin patches. Furthermore, Kim et al. [92] bioprinted cornea grafts using bovine cornea-derived dECM (0.5–2.0%) mixed with human turbinate-derived mesenchymal stem cells (hTMSCs, 1×10^6 cells/mL). *In vitro*, they observed keratocytic differentiation of the encapsulated cells only in the dECM samples, not in the collagen control samples. When implanted in a rabbit corneal pocket, the dECM gels exhibited significantly less immune cell infiltration compared to collagen control samples at day 14 and 28, indicating better immunotolerance of the bovine dECM-based grafts. Interestingly, the dECM gels were more transparent than collagen gels, which was attributed to their thinner fibers resulting from electrostatic forces caused by charged proteoglycans in the dECM.

As an example of further tissue types, Bashiri et al. [77] printed testicular hydrogel constructs using a 3DPL® bioprinter with a biomaterial ink containing 6% gelatin, 6% alginate, and 0–5% testicular dECM. The addition of dECM induced uneven, valley-like surfaces on the hydrogels, and consequently, the attachment of mice spermatogonial stem cells increased with the dECM concentration. However, the

number of cells attached to the dECM-containing scaffolds after 7 and 30 days of subcutaneous transplantation in mice did not differ from the dECM-free control scaffolds. Recently, Chu et al. [59] formulated Schwann cell-laden microgels (1×10^7 cells/mL) using porcine nervous tissue dECM and embedded them in HUVEC-laden GelMA (8% w/v). This composite bioink, filled halfway with the dECM microgels, was pre-gelated at 20 °C and bioprinted using a 3D Bioplotter extrusion printer from EnvisionTEC. The presence of LAP (0.6% w/v) allowed additional photocrosslinking of the final 3D constructs. Compared to directly mixing the cells in GelMA hydrogels, using dECM microgels provided the neuronal cells with a native-like microenvironment and protected them from shear stress during extrusion, thereby increasing their viability.

Furthermore, several groups have explored the use of bioprinted dECM in tumor models. Chen et al. [93]. bioprinted a tumor model using porcine fat-derived dECM mixed with GelMA (1:1) and MFC-7 breast cancer cells (1×10^6 cells/mL) with an extrusion-based Allevi2™ bioprinter. This model was employed for drug-loaded nanoparticle uptake studies. The inclusion of dECM in the bioink allowed fort the simulation of the native ECM barrier in a tumor, a critical factor hindering nanoparticle penetration and reducing drug targeting efficacy. Kort-Mascort et al. [94] bioprinted head and neck tumor models using a GeSiM Bioscaffolder™ 3.1 extrusion printer and bioink comprising porcine tong-derived dECM mixed with alginate, gelatin, and immortalized human squamous carcinoma cells. The resulting 3D hydrogels facilitated the reorganization of cells into tumor spheroids with high viability. Due to the improved representation of native tumor conditions, the efficacy of cancer drugs reduced compared to conventional 2D cell monolayers, leading to more reliable results. In both of these studies above, the inclusion of dECM in the hydrogels enhanced the physiological relevancy of the tumor models, making them more valuable for research purposes.

8. Vat photopolymerized tissue dECM constructs

8.1. Liver dECM constructs

Unlike extrusion bioprinting, which is currently the primary technique for dECM bioprinting, vat photopolymerization often allows for higher resolution dECM bioprinting. Ma et al. [52] used a UV-based DLP printer (365 nm) to photocrosslink thin (200 µm) one-layer patterns of acellular and cellular resins made from unmodified porcine liver dECM (5%) mixed with GelMA (5%) and LAP photoinitiator (0.6%) (Fig. 5A). The inclusion of photocrosslinkable GelMA in the dECM bioink allowed for easy adjustment of material stiffness by varying the light exposure time (10, 20, or 40 s). These gels exhibited stiffness levels of 0.5 kPa (softer than healthy liver tissue), 5 kPa (representative of healthy tissue), and 15 kPa (mimicking cirrhotic tissue). On day 1, the viability of encapsulated HepG2 cells (2.5×10^6 /mL) was consistent across all crosslinked gels, regardless of their stiffness. However, on day 3 and 7, the cell viability decreased significantly in the stiffest constructs designed to mimic cirrhotic tissue. At the same time, migration of the cells increased in these constructs. This observation highlights the importance of considering the mechanical properties of bioprinted dECM hydrogels, as they can significantly impact cellular behavior over time.

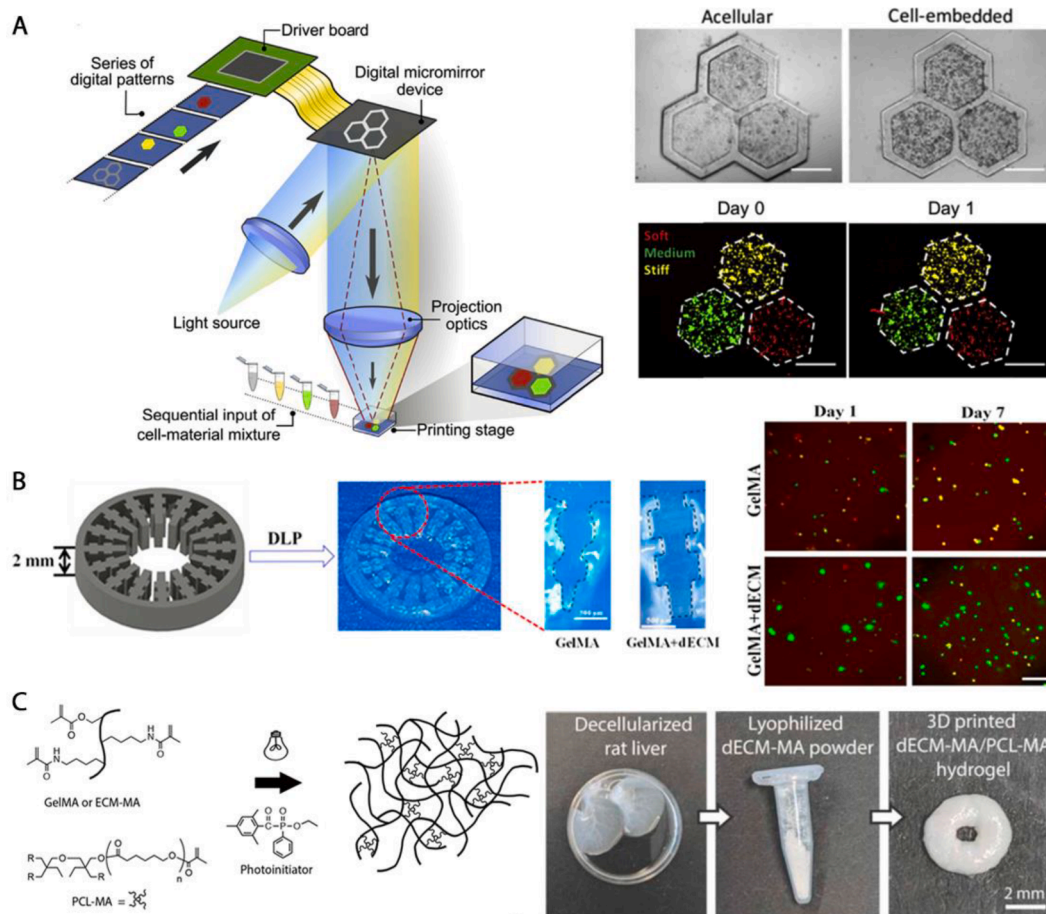In a similar approach, Mao et al. [19] used a UV-based DLP system to

Fig. 5. UV-based DLP bioprinting of (A) immortalized human liver cancer cells-containing porcine liver dECM/GelMA bioink [52] and (B) human hepatocytes-containing porcine liver dECM bioink [19]. (C) Visible light-based DLP printing of multilayered structures of acellular rat liver dECM methacrylamide/PCL methacrylate resin [39]. Reproduced with permission from (A)–(C) Elsevier.

bioprint thicker hydrogel constructs, as depicted in Fig. 5B. Their bio-resin consisted of unmodified porcine liver dECM (3%), GelMA (10%), LAP photoinitiator (0.5%), and human fibroblast-derived induced hepatocytes ($2.5-3 \times 10^6$ cells/mL). To initiate crosslinking, they exposed the samples to UV light at 365 nm with a light intensity of 2.25 mW/cm [2] for duration of 2.5 s. The inclusion of dECM in the bioink led to an enhanced printing resolution compared to cell-laden neat GelMA hydrogels. Furthermore, the dECM promoted the growth of the encapsulated hepatocytes and their ability to secrete albumin and urea nitrogen, demonstrating the beneficial effects of incorporating dECM into the bioink.

While the constructs described above were fabricated using vat photopolymerization, the dECM used in these experiments was chemically unmodified and therefore not part of the covalently crosslinked hydrogel networks. More recently, our group developed an acellular biomaterial ink consisting of methacrylated rat liver dECM (35%) combined with PCL methacrylate (15%) in a diluent comprising formamide and ethyl lactate [39]. By using a visible light DLP printer (Titan 2, Kudo3D) and the LAP (2%) photoinitiator, both polymers in the homogenous formulation were crosslinked into a hybrid network, resulting in the creation of soft yet highly crosslinked multilayered acellular hydrogels (Fig. 5C).

8.2. Other dECM constructs

In addition to liver dECM, we have recently introduced a photo-crosslinkable biomaterial resin based on small intestinal submucosa (dSIS) for vat photopolymerization [32]. This resin was derived from methacrylated solubilized dSIS (dSIS-MA, 1.5%) mixed with 1% LAP photoinitiator, achieving the photocrosslinking kinetics suitable for use with a visible light DLP printer (Titan 2, Kudo3D). The dECM resin was used to 3D print hydrogels that mimicked villi structures found on the luminal side of a native small intestine. Following the printing process, human intestinal organoid-derived primary cells were seeded onto the 3D-printed villi-mimics. Over an 11-day cell culture study, the cells exhibited steady proliferation on the 3D printed villi surface. Eventually, the cells fully covered the surface, forming a mono-layered epithelium replicate, as depicted in Fig. 6A.

In all the previously mentioned studies, photocrosslinking relied on methacrylamide functionalization of dECM or GelMA. Recently, Kim et al. [58] introduced an alternative approach by using the endogenous tyrosine groups present in dECM for covalent crosslinking in the presence of the visible light-sensitive Ru/SPS system. They formulated solubilized porcine heart dECM (1%) in 10 M NaOH supplemented with 1/10 mM Ru/SPS and human bone marrow-derived mesenchymal stem cells (5×10^6 cells/mL). The bioresin was photopolymerized into 3D hydrogels using a LumenX DLP printer (CELLINK) (Fig. 6B). The cell viability in the resulting hydrogels was over 82% after a 24 h cell culture period, indicating good cytocompatibility of this ruthenium-containing dECM bioresin.

9. Biofilm-derived dECM and prokaryotic cell bioprinting

Bacterial communities in biofilms, similar to mammalian cells in tissue and organs, possess their unique ECM known as extracellular polymeric substances (EPS). However, EPS differs from mammalian ECM in terms of its composition and functions. The primary constituents of EPS include exopolysaccharides, such as cellulose, hyaluronic acid, alginate, curdlan, and dextran. Additionally, EPS comprises proteins, extracellular DNA, lipids, lipopolysaccharides, and minerals. These components collectively contribute to the biofilm's ability to main structural integrity [1]. The precise control over spatial and temporal organization achieved through microbial bioprinting offers the opportunity to optimize the assembly of individual bacterial strains,
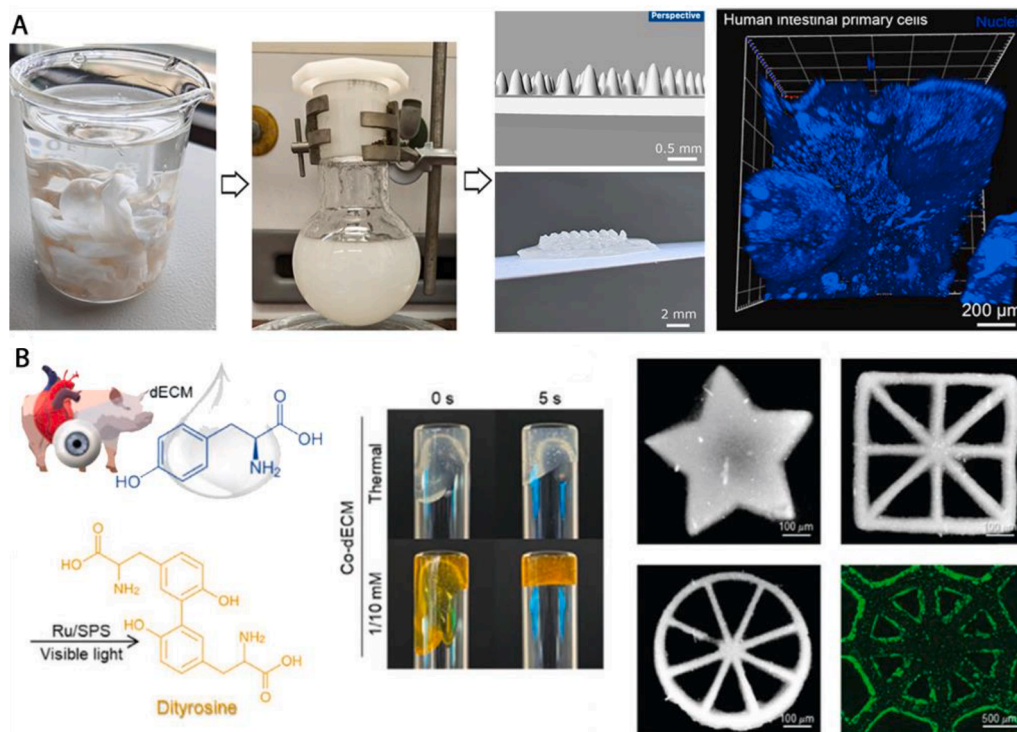

Fig. 6. (. A) Images of decellularized small intestine and the digested dSIS in a flask and DLP printed small intestinal dSIS-based hydrogels with biomimicking villi-structures and nuclei-stained human primary intestinal epithelial cells seeded on the top surface [32]. (B) Schematic drawing of dityrosine crosslinking chemistry and images of thermally and covalently crosslinked dECM hydrogels as well as DLP printed hydrogel constructs of heart dECM (1 %) photocrosslinked via tyrosine groups in the dECM using 1/10 mM Ru/SPS photoinitiator. The hydrogels were bioprinted with human bone marrow mesenchymal stem cells (5×10^6 cells/mL) [58]. Reproduced with permission from (A) Elsevier, (B) John Wiley and Johns.

harnessing their collaborative potential in synthetic biology. While initial microbial bioprinting efforts primarily utilized bioinks composed of alginate, mammalian ECM components, or blends thereof, [95] recent developments have shifted the focus toward formulating bacteria within their self-produced, sustainable matrix. This approach aims to enhance bacterial proliferation, communication, and overall performance within the bioprinted structures.

Creating individual microbial bioinks offers a way to customize the bioink properties for specific applications. An innovative approach involves genetically engineered *E.coli* to produce an ink inspired by fibrin, which is based on self-assembling nanofibers. This study, conducted by Duraj-Thatte et al. [96] aimed at development of genetically modified microbes for 3D bioprinting of programmable and functional living materials. The genetic engineering of microbes to generate their ink is a step toward sustainable ink production. Decellularized microbial inks can be obtained from biofilms by breaking down the bacterial cell wall or membrane using strong denaturants, such as guanidinium chloride or surfactants [96]. Subsequent treatment with nucleases removes bacterial DNA. In the case of decellularized engineered *E. coli* biofilms, amyloid fiber precursors can be isolated on a filter through washing and subsequently gelated into nanofibrous hydrogels, for instance, through SDS treatment [96]. Alternatively, extraction of biofilms in the presence of sodium chloride effectively isolates solubilized EPS components after centrifugation, with minimal impact on the viability of both gram-negative and gram-positive strains. Consequently, the resulting preparations contain fewer contaminants from intracellular proteins and can be further chemically modified for bioprinting. While sterilizing microbial inks has not been systematically addressed yet, the long-term culture of printed bacteria-containing constructs faces similar challenges to those with mammalian cells. The primary challenge is preventing microbial contamination while maintaining the viability and functionality of the desired bacterial cells and preserving the structural integrity of the bioprinted constructs. Despite these challenges, the field of microbial cell bioprinting holds great promise, especially with advancements in synthetic biology, and new innovate ways to harness their potential are continuously explored.

10. Future directions in dECM-based bioprinting

The field of 3D bioprinting has evolved from being a niche area to becoming a common tool in biomaterial science, thanks to its widespread availability. However, despite the increasing development of new dECM-based bioinks, the protocols for their preparation have not seen significant improvements in recent years. This is particularly evident in the solubilization step. The dECM is nearly exclusively solubilized using pepsin-based enzymatic digestion, whereas other potentially more cost-effective or non-animal-derived enzymes have been overlooked. There is a clear need for a comprehensive comparison of different enzymes, focusing on their digestion sites within dECM and their impact on the bioprinting properties of the resulting materials. In essence, a more systematic evaluation of enzyme choices is required to optimize the solubilization process. Moreover, standardization of protocols for all stages of dECM hydrogel production is essential. The absence of such standardized protocols makes it challenging to systematically compare and evaluate different studies in the topic.

In most non-human dECM-based formulations, the dECM content typically ranges from 1% to 5% dECM. In cases where scarcely available human dECM is used, a lower amount of dECM is often mixed with other polymers [88]. To fully harness the potential of bioprinted humanized dECM hydrogels, it is crucial to determine the critical amount of human dECM needed for detectable bioactivity. Additionally, more comparative studies are required to establish correlations between the dECM composition and its biological response. Further research should focus on conducting comprehensive biological evaluations of the printed constructs under extended biomimicking culture conditions. Specifically, it is important to investigate whether tissue-specific dECM is

necessary or if certain dECM types can support a broader range of cell types effectively. Additionally, it is essential to assess the true bioactivity of dECM hydrogels by carefully analyzing cell functions in comparison to gelatin and collagen controls, where tissue-specific compounds are absent. Currently, bioprinted dECM constructs are valuable for improving 3D *in vitro* tissue models, enabling better understanding of cell behavior. However, for the development of transplantable functional bioprinted tissues, it is imperative to thoroughly investigate the immunogenicity and safety of bioprinted dECM-based materials.

To advance vat photopolymerization of dECM-based resins, exploring new methods for chemically functionalizing dECM could offer improvements in printing resolution while maintaining high cell viability. Currently, the most extensively studied approach involves methacrylate-functionalized dECM, with some preliminary research into tyrosine crosslinking chemistry, while other functional groups remain to be applied to dECM. One potential avenue could be thiol-ene photopolymerization, which is known to be less susceptible to oxygen inhibition than methacrylate chemistry [97]. This means that fewer radicals are required to initiate polymerization, reducing the risk of radical-induced damage to cells and enhancing the bioprinting capabilities of dECM. Furthermore, advancements in 3D printing techniques can significantly improve the printability of soft dECM-based hydrogels. Achieving a balance between the crosslinking density that is favorable for cell viability and high printing resolution is crucial. One approach gaining particular attention is the Freeform Reversible Embedding of Suspended Hydrogels (FRESH) technique, where the bioink is extruded into a support bath rather than an open-air environment [98]. When applied to dECM-based bioinks, this technique can enable bioprinting of precise anatomical structures, such as perfusable vasculature or bifurcating airways, as demonstrated in the preliminarily studies [61].

11. Conclusions

ECM is typically decellularized using the sequential SDS/Triton™ X-100 treatment because it effectively removes cellular components while sufficiently preserving essential biomolecules. For the solubilization of dECM, papain can be recommended as a cost-effective plant-derived enzyme that results in consistent dECM pre-gels suitable for extrusion bioprinting. The dECM pre-gels can be further chemically modified for the use as bioinks in light-assisted extrusion printing or as bioresins in vat photopolymerization. However, applying ruthenium-initiated photocrosslinking on unmodified dECM eliminates the need for an additional processing step, potentially preserving essential bioactive molecules. Despite the research on the effects of various processing methods on the physicochemical and biological properties of dECM, ideal protocols remain elusive because of the incomparability of these studies. Therefore, more comparative studies are needed to better understand how processing parameters influence material properties and to develop optimized protocols with organ- and species-specific adaptations reflecting individual tissue composition, anatomy, and history. For standardization, especially rheological tests are crucial, as the viscosity indirectly reveals the degree of dECM digestion and significantly affects bioprinting results, as discussed in this review. Developing more unified processing and characterization steps for dECM-based bioinks and bioresins will ultimately lead to the rational utilization of their unique properties in future bioprinting of both mammalian and bacterial cell constructs.

Declaration of Competing Interest

The authors declare that they have no known competing financial interests or personal relationships that could have appeared to influence the work reported in this paper.

Data availability

No data was used for the research described in the article.

Acknowledgments

References

[1] Balasubramanian S, Yu K, Cardenas DV, Meyer AS. Emergent biological endurance depends on extracellular matrix composition of three-dimensionally printed *Escherichia coli* biofilms. ACS Synth Biol 2021;10:2997.

[2] Kim BS, Das S, Jang J, Cho D. Decellularized extracellular matrix-based bioinks for engineering tissue- and organ-specific microenvironments. Chem Rev 2020;120: 10608.

[3] Yao Q, Zheng YW, Lan QH, Kou L, Xu HL, Zhao YZ. Recent development and biomedical applications of decellularized extracellular matrix biomaterials. Mater Sci Eng C 2019;104:109942.

[4] Han W, Singh NK, Kim JJ, Kim H, Kim BS, Park JY, Jang J, Cho DW. Directed differential behaviors of multipotent adult stem cells from decellularized tissue/ organ extracellular matrix bioinks. Biomaterials 2019;224:119496.

[5] Dzobo K, Motaung KSCM, Adesida A. Recent trends in decellularized extracellular matrix bioinks for 3D printing: an updated review. Int J Mol Sci 2019;20:4628.

[6] Zhang YS, Haghiashtiani G, Kelly DJ, Yeong WY, Lee JM, Lutolf M, Mcalpine MC, Zenobi M, Malda J. 3D extrusion bioprinting. Nat Rev Methods Prim 2021;1:1.

[7] Zhang F, Zhu L, Li Z, Wang S, Shi J, Tang W, Li N, Yang J. The recent development of vat photopolymerization: a review. Addit Manuf 2021;48:102423.

[8] Groll J, Burdick JA, Cho DW, Derby B, Gelinsky M, Heilshorn SC, Jüngst T, Malda J, Mironov VA, Nakayama K, Ovsianikov A, Sun W, Takeuchi S, Yoo JJ, Woodfield TBF. A definition of bioinks and their distinction from biomaterial inks. Biofabrication 2018;11:013001.

[9] Kasravi M, Ahmadi A, Babajani A, Mazloomnejad R. Immunogenicity of decellularized extracellular matrix scaffolds : a bottleneck in tissue engineering and regenerative medicine. Biomater Res 2023;27:1.

[10] Crapo PM, Gilbert TW, Badylak SF. An overview of tissue and whole organ decellularization processes. Biomaterials 2012;32:3233.

[11] Hillebrandt KH, Everwien H, Haep N, Keshi E, Pratschke J, Sauer IM. Strategies based on organ decellularization and recellularization. Transpl Int 2019;32:571.

[12] Guimaraes AB, Correia AT, Alves BP, Da Silva RS, Martins JK, Pêgo-Fernandes PM, Xavier NS, Dolhnikoff M, Cardoso PFG. Evaluation of a physical-chemical protocol for porcine tracheal decellularization. Transplant Proc 2019;51:1611.

[13] Yusof F, Sha'ban M, Azhim A. Development of decellularized meniscus using closed sonication treatment system: potential scaffolds for orthopedics tissue engineering applications. Int J Nanomed 2019;14:5491.

[14] Bakhtiar H, Rajabi S, Pezeshki-Modaress M, Ellini MR, Panahinia M, Alijani S, Mazidi A, Kamali A, Azarpazhooh A, Kishen A. Optimizing methods for bovine dental pulp decellularization. J Endod 2021;47:62.

[15] Shahraki S, Bideskan AE, Mohammad A, Tavakkoli M, Bahrami AR, Hosseinian S, Matin MM, Rad AK. Decellularization with triton X-100 provides a suitable model for human kidney bioengineering using human mesenchymal stem cells. Life Sci 2022;295:120167.

[16] Jeong W, Kim CM, Kang HW. Effect of detergent type on the performance of liver decellularized extracellular matrix-based bio-inks. J Tissue Eng 2021;12:1.

[17] Higuita ML, Griffiths LG, Clinic M, Clinic M. Antigen removal process preserves function of small diameter venous valved conduits, whereas SDS-decellularization results in significant valvular insufficiency. Acta Biomater 2020;107:115.

[18] Kim YS, Majid M, Melchiorri AJ, Mikos AG. Applications of decellularized extracellular matrix in bone and cartilage tissue engineering. Bioeng Transl Med 2019;4:83.

[19] Mao Q, Wang Y, Li Y, Juengpanich S, Li W, Chen M, Yin J, Fu J, Cai X. Fabrication of liver microtissue with liver decellularized extracellular matrix (dECM) bioink by digital light processing (DLP) bioprinting. Mater Sci Eng C 2020;109:110625.

[20] Gilpin A, Yang Y. Decellularization strategies for regenerative medicine: from processing techniques to applications. BioMed Res Int 2017;2017:1.

[21] McCrary M, Vaughn NE, Hlavac N, Song YH, Wachs RA, Schmidt CE. Novel sodium deoxycholate - based chemical decellularization method for peripheral nerve. Tissue Eng Part C 2020;26:1.

[22] Fernández-Pérez J, Ahearne M. The impact of decellularization methods on extracellular matrix derived hydrogels. Sci Rep 2019;9:1.

[23] Lunney JK, Van Goor A, Walker KE, Hailstock T, Franklin J, Dai C. Importance of the pig as a human biomedical model. Sci Transl Med 2021;13:1.

[24] Guimarães CF, Gasperini L, Marques AP, Reis RL. The stiffness of living tissues and its implications for tissue engineering. Nat Rev Mater 2020;5:351.

[25] Voytik-Harbin SL, Brightman AO, Waisner BZ, Robinson JP, Lamar CH. Small intestinal submucosa: a tissue-derived extracellular matrix that promotes tissue-specific growth and differentiation of cells *in vitro*. Tissue Eng 1998;4:157.

[26] Luo Q, Chen D, Boom RM, Janssen AEM. Revisiting the enzymatic kinetics of pepsin using isothermal titration calorimetry. Food Chem 2018;268:94.

[27] Pouliot RA, Young BM, Link PA, Park HE, Kahn AR, Shankar K, Schneck MB, Weiss DJ, Heise RL. Physical, mechanical, and bioactive properties of pig lung-derived ECM hydrogels are dependent on the duration of pepsin digestion. Tissue Eng Part C Methods 2020;26:332.

[28] Almalla A, Elomaa L, Bechtella L, Daneshgar A, Yavvari P, Mahfouz Z, et al. Papain-based solubilization of decellularized extracellular matrix for the preparation of bioactive, thermosensitive pre-gels. Biomacromolecules 2023. https://doi.org/10.1021/acs.biomac.3c00602.

[29] Hong H, Fan H, Roy BC, Wu J. Amylase enhances production of low molecular weight collagen peptides from the skin of spent hen, bovine, porcine, and tilapia. Food Chem 2021;352:129355.

[30] Jia L, Hua Y, Zeng J, Liu W, Wang D, Zhou G, Liu X, Jiang H. Bioprinting and regeneration of auricular cartilage using a bioactive bioink based on microporous photocrosslinkable acellular cartilage matrix. Bioact Mater 2022;16:66.

[31] Kornmuller A, Brown CFC, Yu C, Flynn LE. Fabrication of extracellular matrix-derived foams and microcarriers as tissue-specific cell culture and delivery platforms. J Vis Exp 2017;122:55436.

[32] Elomaa L, Gerbeth L, Almalla A, Fribiczer N, Daneshgar A, Tang P, et al. Bioactive photocrosslinkable resin solely based on refined decellularized small intestine submucosa for vat photopolymerization of *in vitro* tissue mimics. Addit Manuf 2023;64:103439.

[33] Kiyotake EA, Cheng ME, Thomas EE, Detamore MS. The rheology and printability of cartilage matrix-only biomaterials. Biomolecules 2022;12:846.

[34] Visscher DO, Lee H, van Zuijlen PPM, Helder MN, Atala A, Yoo JJ, Lee SJ. A photo-crosslinkable cartilage-derived extracellular matrix (ECM) bioink for auricular cartilage tissue engineering. Acta Biomater 2021;121:193.

[35] Visser J, Levett PA, te Moller NCR, Besems J, Boere K, van Rijen MHP, de Grauw JC, Dhert WJ, van Weeren PR, Malda J. Crosslinkable hydrogels derived from cartilage, meniscus, and tendon tissue. Tissue Eng Part A 2015;21:1195.

[36] Rothrauff BB, Coluccino L, Gottardi R, Ceseracciu L, Scaglione S, Goldoni L, Tuan RS. Efficacy of thermoresponsive, photocrosslinkable hydrogels derived from decellularized tendon and cartilage extracellular matrix for cartilage tissue engineering. J Tissue Eng Regen Med 2018;12:e159.

[37] Ali M, PR AK, Yoo JJ, Zahran F, Atala A, Lee SJ. A photo-crosslinkable kidney ECM-derived bioink accelerates renal tissue formation. Adv Healthc Mater 2019;8: 1800992.

[38] Kim W, Lee H, Lee J, Atala A, Yoo JJ, Jin S, Kim GH. Efficient myotube formation in 3D bioprinted tissue construct by biochemical and topographical cues. Biomaterials 2020;230:119632.

[39] Elomaa L, Keshi E, Sauer IM, Weinhart M. Development of GelMA/PCL and dECM/ PCL resins for 3D printing of acellular *in vitro* tissue scaffolds by stereolithography. Mater Sci Eng C 2020;112:110958.

[40] Kiyotake EA, Thomas EE, Iribagiza C, Detamore MS. High-stiffness, fast-crosslinking, cartilage matrix bioinks. J Biomech 2023;148:111471.

[41] Jang J, Park HJJ, Kim SW, Kim HHJ, Park JY, Na SJ, Kim HHJ, Park MN, Choi SH, Park SH, Kim SW, Kwon SMM, Kim PJJ, Cho DWW. 3D printed complex tissue construct using stem cell-laden decellularized extracellular matrix bioinks for cardiac repair. Biomaterials 2017;112:264.

[42] Moradi L, Jobania B, Mohammadi Jafarnezhad-Ansariha F, Ghorbani F, Esmaeil-Pour R, Zolbina MM, Kajbafzadeha AM. Evaluation of different sterilization methods for decellularized kidney tissue. Tissue Cell 2020;66:101396.

[43] Yaldiz B, Saglam-Metiner P, Cam SB, Korkusuz P, Yesil-Celiktas O. Effect of sterilization methods on the mechanical stability and extracellular matrix constituents of decellularized brain tissues. J Supercrit Fluids 2021;175:105299.

[44] O'Connell CD, Onofrillo C, Duchi S, Li X, Zhang Y, Tian P, Lu L, Trengove A, Quigley A, Gambhir S, Khansari A, Mladenovska T, O'Connor A, Di Bella C, Choong PF, Wallace GG. Evaluation of sterilisation methods for bio-ink components: gelatin, gelatin methacryloyl, hyaluronic acid and hyaluronic acid methacryloyl. Biofabrication 2019;11:35003.

[45] Kim BS, Kwon YW, Kong JS, Park GT, Gao G, Han W, Kim MB, Lee H, Kim JH, Cho DW. 3D cell printing of *in vitro* stabilized skin model and *in vivo* pre-vascularized skin patch using tissue-specific extracellular matrix bioink: a step towards advanced skin tissue engineering. Biomaterials 2018;168:38.

[46] Chae S, Kim J, Yi HG, Cho DW. 3D bioprinting of an *in vitro* model of a biomimetic urinary bladder with a contract-release system. Micromachines 2022;13:277.

[47] Kim WJ, Kim GH. An intestinal model with a finger-like villus structure fabricated using a bioprinting process and collagen/SIS-based cell-laden bioink. Theranostics 2020;10:2495.

[48] Yu C, Ma X, Zhu W, Wang P, Miller KL, Stupin J, Koroleva-Maharajh A, Hairabedian A, Chen S. Scanningless and continuous 3D bioprinting of human tissues with decellularized extracellular matrix. Biomaterials 2019;194:1.

[49] Ribeiro N, Soares GC, Santos-Rosales V, Concheiro A, Alvarez-Lorenzo C, Garcia-Gonzalez CA, Oliveira AL. A new era for sterilization based on supercritical CO$_2$ technology. J Biomed Mater Res B Appl Biomater 2020;108:399.

[50] Hull CW. Apparatus for Production of Three-Dimensional Objects by Stereolithography (US4575330). San Gabriel, California: UVP, Inc; 1986.

[51] Wilson WC, Boland T. Cell and organ printing 1: protein and cell printers. Anat Rec 2003;272:491.

[52] Ma X, Yu C, Wang P, Xu W, Wan X, Lai CSE, Liu J, Koroleva-Maharajh A, Chen S. Rapid 3D bioprinting of decellularized extracellular matrix with regionally varied mechanical properties and biomimetic microarchitecture. Biomaterials 2018;185: 310.

[53] Shin YJ, Shafranek RT, Tsui JH, Walcott J, Nelson A, Kim DH. 3D bioprinting of mechanically tuned bioinks derived from cardiac decellularized extracellular matrix. Acta Biomater 2021;119:75.

[54] Leo L, Bridelli MG, Polverini E. Biophysical Chemistry Insight on collagen self-assembly mechanisms by coupling molecular dynamics and UV spectroscopy techniques. Biophys Chem 2019;253:106224.

[55] Yang K, Sun J, Wei D, Yuan L, Yang J, Guo L, Fan H, Zhang X, Fan H, Yang J, Sun J, Yang K, Guo L, Yuan L, Sun J, Wei D, Yuan L, Yang J, Guo L, Fan L, Zhang X. Photo-crosslinked mono-component type II collagen hydrogel as a matrix to induce chondrogenic differentiation of bone marrow mesenchymal stem cells. J Mater Chem B 2017;5:8707.

[56] Rothrauff BB, Coluccino L, Gottardi R, Ceseracciu L, Scaglione S, Goldoni L, Tuan RS. Matrix for cartilage tissue engineering. J Tissue Eng Regen Med 2018;12:1.

[57] Zhang T, Chen H, Zhang Y, Zan Y, Ni T, Liu M, Pei R. Photo-crosslinkable, bone marrow-derived mesenchymal stem cells-encapsulating hydrogel based on collagen for osteogenic differentiation. Colloids Surf B Biointerfaces 2019;174:528.

[58] Kim H, Kang B, Cui X, Lee SH, Lee K, Cho DW, Hwang W, Woodfield TBF, Lim KS, Jang J. Light-activated decellularized extracellular matrix-based bioinks for volumetric tissue analogs at the centimeter scale. Adv Funct Mater 2021;31:2011252.

[59] Chu H, Zhang K, Rao Z, Song P, Lin Z, Zhou J, Yang L. Harnessing decellularised extracellular matrix microgels into modular bioinks for extrusion-based bioprinting with good printability and high post-printing cell viability. Biomater Transl 2023;4:115.

[60] Basara G, Gulberk Ozcebe S, Ellis BW, Zorlutuna P. Tunable human myocardium derived decellularized extracellular matrix for 3D bioprinting and cardiac tissue engineering. Gels 2021;7:70. Page7, 70, 2021.

[61] De Santis MM, Alsafadi HN, Tas S, Bölükbas DA, Prithiviraj R, Da Silva IAN, Mittendorfer M, Ota C, Stegmayr J, Daoud F, Königshoff M, Swärd K, Wood JA, Tassieri M, Bourgine PE, Lindstedt S, Mohlin S, Wagner DE. Extracellular-matrix-reinforced bioinks for 3D bioprinting human tissue. Adv Mater 2021;33:2005476.

[62] Schwartz R, Malpica M, Thompson GL, Miri AK. Cell encapsulation in gelatin bioink impairs 3D bioprinting resolution. J Mech Behav Biomed Mater 2020;103:103524.

[63] Schwab A, Levato R, D'Este M, Piluso S, Eglin D, Malda J. Printability and shape fidelity of bioinks in 3D bioprinting. Chem Rev 2020;120:11028.

[64] Diamantides N, Dugopolski C, Blahut E, Kennedy S, Bonassar LJ. High density cell seeding affects the rheology and printability of collagen bioinks. Biofabrication 2019;11:045016.

[65] Sun W, Starly B, Daly AC, Burdick JA, Groll J, Skeldon G, Shu W, Sakai Y, Shinohara M, Nishikawa M, Jang J, Cho DW, Nie M, Takeuchi S, Ostrovidov S, Khademhosseini A, Kamm RD, Mironov V, Moroni L, Ozbolat IT. The bioprinting roadmap. Biofabrication 2020;12:022002.

[66] Ahn G, Min KHH, Kim C, Lee JSS, Kang D, Won JYY, Cho DWW, Kim JYY, Jin S, Yun WSS, Shim JHH. Precise stacking of decellularized extracellular matrix based 3D cell-laden constructs by a 3D cell printing system equipped with heating modules. Sci Rep 2017;8:8624.

[67] Choi YJ, Jun YJ, Kim DY, Yi HG, Chae SH, Kang J, Lee J, Gao G, Kong JS, Jang J, Chung WK, Rhie JW, Cho DW. A 3D cell printed muscle construct with tissue-derived bioink for the treatment of volumetric muscle loss. Biomaterials 2019;206:160.

[68] Idaszek J, Volpi M, Paradiso A, Nguyen Quoc M, Górecka Ż, Klak M, Tymicki G, Berman A, Wierzbicki M, Jaworski S, Costantini M, Kępczyńska A, Chwalibóg ES, Wszoła M, Święszkowski W. Alginate-based tissue-specific bioinks for multi-material 3D-bioprinting of pancreatic islets and blood vessels: a step towards vascularized pancreas grafts. Bioprinting 2021;24:e00163.

[69] Yang X, Ma Y, Wang X, Yuan S, Huo F, Yi G, et al. A 3D-bioprinted functional module based on decellularized extracellular matrix bioink for periodontal regeneration. Adv Sci 2023;10:2205041.

[70] Toprakhisar B, Nadernezhad A, Bakirci E, Khani N, Skvortsov GA, Koc B. Development of bioink from decellularized tendon extracellular matrix for 3D bioprinting. Macromol Biosci 2018;18:1800024.

[71] Zhao F, Cheng J, Sun M, Yu H, Wu N, Li Z, et al. Digestion degree is a key factor to regulate the printability of pure tendon decellularized extracellular matrix bio-ink in extrusion-based 3D cell printing. Biofabrication 2020;12:045011.

[72] Ruskowitz ER, Deforest CA. Proteome-wide analysis of cellular response to ultraviolet light for biomaterial synthesis and modification. ACS Biomater Sci Eng 2019;5:2111.

[73] Rizzo R, Petelinšek N, Bonato A, Zenobi-Wong M. From free-radical to radical-free: a paradigm shift in light-mediated biofabrication. Adv Sci 2023;10:2205302.

[74] Xu H, Casillas J, Krishnamoorthy S, Xu C. Effects of Irgacure 2959 and lithium phenyl-2,4,6-trimethylbenzoylphosphinate on cell viability, physical properties, and microstructure in 3D bioprinting of vascular-like constructs. Biomed Mater 2020;15:055021.

[75] Park HK, Shin M, Kim B, Park JW, Lee H. A visible light-curable yet visible wavelength-transparent resin for stereolithography 3D printing. NPG Asia Mater 2018;10:82.

[76] Uemura R, Miura J, Ishimoto T, Yagi K, Matsuda Y, Shimizu M, et al. UVA-activated riboflavin promotes collagen crosslinking to prevent root caries. Sci Rep 2019;9:1252.

[77] Bashiri Z, Amiri I, Gholipourmalekabadi M, Falak R, Asgari H, Maki CB, Moghaddaszadeh A, Koruji M. Artificial testis: a testicular tissue extracellular matrix as a potential bio-ink for 3D printing. Biomater Sci 2021;9:3465.

[78] Kim J, Kim M, Hwang DG, Shim IK, Kim SC, Jang J. Pancreatic tissue-derived extracellular matrix bioink for printing 3D cell-laden pancreatic tissue constructs. J Vis Exp 2019;154:60434.

[79] Paxton N, Smolan W, Böck T, Melchels F, Groll J, Jungst T. Proposal to assess printability of bioinks for extrusion-based bioprinting and evaluation of rheological properties governing bioprintability. Biofabrication 2017;9:044107.

[80] Townsend J, Beck E, Gehrke S, Berkland C, Detamore M. Flow behavior prior to crosslinking: the need for precursor rheology for placement of hydrogels in medical applications and for 3D bioprinting. Prog Polym Sci 2019;91:126.

[81] Gao T, Gillispie GJ, Copus JS, Pr AK, Seol Y. Optimization of gelatin – alginate composite bioink printability using rheological parameters : a systematic approach Optimization of gelatin – alginate composite bioink printability using rheological parameters : a systematic approach. Biofabrication 2018;10:034106.

[82] Ribeiro A, Blokzijl MM, Levato R, Visser CW, Castilho M, Hennink WE, et al. Assessing bioink shape fidelity to aid material development in 3D bioprinting. Biofabrication 2018;10:014102.

[83] Sun T, Meng C, Ding Q, Yu K, Zhang X, Zhang W, Tian W, Zhang Q, Guo X, Wu B, Xiong Z. In situ bone regeneration with sequential delivery of aptamer and BMP2 from an ECM-based scaffold fabricated by cryogenic free-form extrusion. Bioact Mater 2021;6:4163.

[84] Chae S, Yong U, Park W, Choi Ymi, Jeon IH, Kang H, Jang J, Choi HS, Cho DW. 3D cell-printing of gradient multi-tissue interfaces for rotator cuff regeneration. Bioact Mater 2023;19:611.

[85] Bin Y, Dongzhen Z, Xiaoli C, jirigala E, Wei S, Zhao L, Tian H, Ping Z, Jianjun L, Yuzhen W, Yijie Z, Xiaobing F, Sha H. Modeling human hypertrophic scars with 3D preformed cellular aggregates bioprinting. Bioact Mater 2022;10:247.

[86] Pati F, Jang J, Ha DHH, Won Kim S, Rhie JWW, Shim JHH, Kim DHH, Cho DWW. Printing three-dimensional tissue analogues with decellularized extracellular matrix bioink. Nat Commun 2014;5:1.

[87] Lee H, Han W, Kim H, Ha DH, Jang J, Kim BS, Cho DW. Development of liver decellularized extracellular matrix bioink for three-dimensional cell printing-based liver tissue engineering. Biomacromolecules 2017;18:1229.

[88] Hiller T, Berg J, Elomaa L, Röhrs V, Ullah I, Schaar K, Dietrich AC, Al-Zeer M, Kurtz A, Hocke A, Hippenstiel S, Fechner H, Weinhart M, Kurreck J. Generation of a 3D liver model comprising human extracellular matrix in an alginate/gelatin-based bioink by extrusion bioprinting for infection and transduction studies. Int J Mol Sci 2018;19:3129.

[89] Kim J, Shim IK, Hwang DG, Lee YN, Kim M, Kim H, Kim SW, Lee S, Kim SC, Cho DW, Jang J. 3D cell printing of islet-laden pancreatic tissue-derived extracellular matrix bioink constructs for enhancing pancreatic functions. J Mater Chem B 2019;7:1773.

[90] Behan K, Dufour A, Garcia O, Kelly D. Methacrylated cartilage ECM-based hydrogels as injectables and bioinks for cartilage tissue engineering. Biomolecules 2022;12:216.

[91] Zhang X, Liu Y, Luo C, Zhai C, Li Z, Zhang Y, Yuan T, Dong S, Zhang J, Fan W. Crosslinker-free silk/decellularized extracellular matrix porous bioink for 3D bioprinting-based cartilage tissue engineering. Mater Sci Eng C 2021;118:111388.

[92] Kim H, Park MN, Kim J, Jang J, Kim HK, Cho DW. Characterization of cornea-specific bioink: high transparency, improved in vivo safety. J Tissue Eng 2019;10:1.

[93] Chen Y, Xu L, Li W, Chen W, He Q, Zhang X, et al. 3D bioprinted tumor model with extracellular matrix enhanced bioinks for nanoparticle evaluation. Biofabrication 2022;14:025002.

[94] Kort-Mascort J, Bao G, Elkashty O, Flores-Torres S, Munguia-Lopez JG, Jiang T, Ehrlicher AJ, Mongeau L, Tran SD, Kinsella JM. Decellularized extracellular matrix composite hydrogel bioinks for the development of 3D bioprinted head and neck in vitro tumor models. ACS Biomater Sci Eng 2021;7:5288.

[95] Schaffner M, Rühs PA, Coulter F, Kilcher S, Studart AR. 3D printing of bacteria into functional complex materials. Sci Adv 2017;3:eaao6804.

[96] Duraj-Thatte AM, Courchesne ND, Praveschotinunt P, Rutledge J, Lee Y, Karp JM, et al. Genetically programmable self-regenerating bacterial hydrogels. Adv Mater 2019;1:1901826.

[97] Göckler T, Haase S, Kempter X, Pfister R, Maciel BR, Grimm A, et al. Tuning superfast curing thiol-norbornene-functionalized gelatin hydrogels for 3D bioprinting. Adv Healthcare Mater 2021;10:2100206.

[98] Shiwarski DJ, Hudson AR, Tashman JW, Feinberg AW. Emergence of FRESH 3D printing as a platform for advanced tissue biofabrication. APL Bioeng 2021;5:10904.